Atmospheric Research 252 (2021) 105450

Contents lists available at ScienceDirect

Atmospheric Research

journal homepage: www.elsevier.com/locate/atmosres

Groups of narrow bipolar events within thunderstorms

Sampath Bandara, Thomas Marshall *, Sumedhe Karunarathne [1], Maribeth Stolzenburg

Department of Physics & Astronomy, University of Mississippi, University, MS 38677, USA

ARTICLE INFO

Keywords:
Lightning
Thunderstorm
Narrow bipolar event
Compact intracloud discharge
NBE
CID

ABSTRACT

This investigation is focused on groups of Narrow Bipolar Events (NBEs), defined as NBEs that occurred within 10 km horizontally and ±660 ms of a located, large-amplitude NBE from a dataset of positive NBEs that occurred in Mississippi thunderstorms. In two months only 15 groups were found, with a total of 31 positive and 4 negative NBEs. Each group had 2 to 5 NBEs; four groups had both positive and negative polarity NBEs. About half of the NBEs had typical values for range-normalized fast antenna (FA) electric field change magnitudes (4–15 V/m) and typical VHF powers (1000–45,000 W), but 17 NBEs had FA magnitudes 0.2–2.5 V/m, and 17 NBEs had VHF powers 30–900 W. Seven weak NBEs had FA magnitudes of 0.2–1.0 V/m and VHF powers of 30–100 W. These findings indicate that weak NBEs are more common than previously thought. None of the NBEs in groups initiated a lightning flash, and (with one possible exception) none of the later NBEs in a group were initiated by earlier NBEs in the group. The data of the NBE groups are consistent with the turbulence-extensive air shower (EAS)/relativistic runaway electron avalanche (RREA) mechanism, which states that each NBE occurs in a separate 1-km^3 volume containing many small regions with electric field $\geq$3 MV/(m•atm); an EAS/RREA passing through the 1-km^3 volume initiates the positive streamers that comprise the NBE. Relative to thunderstorm radar reflectivity, 23 NBEs occurred in or above the reflectivity core, 10 NBEs occurred high in the storm anvil, and 2 NBEs occurred beside the storm core. We speculate that the occurrence of many of the NBE groups was associated with dynamically intense convection.

1. Introduction

Narrow Bipolar Events (NBEs) are short duration (~20–30 μs) lightning discharge events that are the "sources of the strongest radio frequency radiation from lightning" in the HF-VHF radio bands of 3–300 MHz (Le Vine, 1980). NBEs are typically detected with electric field change (*E*-change) sensors called "fast antennas" or FAs herein; FAs typically operate in some portion of the 0.1 Hz – 3 MHz frequency range. NBEs are also known by various other names, including "compact intracloud discharges" or CIDs because of their relatively short lengths (< 1000 m) (e.g., Smith et al., 1999; Nag et al., 2010) and "narrow bipolar pulses" or NBPs, which describe their far field waveforms detected with FAs (e.g., Smith et al., 2002).

NBEs can have either positive or negative polarity based on the polarity of the leading pulse in the bipolar waveform plotted using the physics convention for electric field polarity (Willett et al., 1989). It is now thought that NBEs are caused by a large number of almost simultaneous positive streamer flashes (e.g., Rison et al., 2016; Kostinskiy et al., 2020a). Thus, positive NBPs are produced by positive charges moving downward (due to a downward pointing electric field) leaving negative charges along the path, while negative NBEs are caused by positive charges moving upward (due to an upward pointing electric field) leaving negative charges along the path (Karunarathne et al., 2015).

All NBEs were originally thought to be isolated from each other and from typical cloud-to-ground (CG) lightning flashes and intracloud (IC) lightning flash activities (e.g., Le Vine, 1980; Willett et al., 1989; Smith et al., 1999); such NBEs are called "Isolated" NBEs herein. However, positive NBEs are now known to initiate some IC flashes (e.g., Rison et al., 1999; Nag et al., 2010; Wu et al., 2014; Karunarathne et al., 2015; Rison et al., 2016; Lyu et al., 2019), and negative NBEs are known to initiate some CG flashes (Rison et al., 2016; Bandara et al., 2019). These NBEs are called "Initiator" NBEs or INBEs herein. In addition, some NBEs occur during the time of and in the vicinity of CG or IC flashes but do not initiate these flashes (Nag et al., 2010; Karunarathne et al., 2015; Bandara et al., 2020), and are called "Not-Isolated" NBEs herein.

* Corresponding author.
E-mail address: marshall@olemiss.edu (T. Marshall).
[1] Present address: FedEx Business Intelligence and Analytics Services, 3620 Hacks Cross Rd., Memphis, TN 38125, USA.

https://doi.org/10.1016/j.atmosres.2021.105450
Received 23 August 2020; Received in revised form 30 December 2020; Accepted 1 January 2021
Available online 6 January 2021

Using an array of three FAs, an array of three HF (3–30 MHz) receivers, and National Weather Service radar data, Smith et al. (1999) studied positive NBEs and found that they tend to occur as isolated events "in close spatial proximity to the very high reflectivity regions of thunderstorms." Wiens et al. (2008) statistically compared NBE discharge rates and ordinary lightning flash rates to the convective strength of thunderstorms inferred from radar data and concluded that "although NBEs do occur in the same storms as ordinary lightning, NBE rate is not broadly proportional to total lightning rate nor to convective strength. Rather…NBEs are more prevalent in the strongest convection." Wu et al. (2013) studied the location of NBE discharges in relation to thunderstorm structure using a phased array radar in the Osaka region of Japan and found that NBEs "generally" occurred in the strongest convection, but in some storms extending above 15 km altitude, positive NBEs occurred around rather than within the strongest convection. Furthermore, they observed that positive NBEs usually occurred well within the thundercloud, while negative NBEs usually occurred close to the upper boundary of a thundercloud. Starting with 226 positive NBEs identified by Karunarathne et al. (2015) in Florida thunderstorms, Karunarathna et al. (2015) analyzed the locations of 172 positive NBEs relative to radar data and determined that these NBEs all occurred within or at the edge of the radar reflectivity. Karunarathna et al. (2015) found that 79% of the positive NBEs occurred in or above the high-reflectivity core while 17% were found beside the reflectivity core. The remaining NBEs (4%) occurred in the anvil region of storms. Herein we also study the radar location of each NBE in the NBE groups.

Based on balloon electric field measurements in thunderstorms, a typical charge distribution in the storm updraft has (from bottom to top) four horizontally extensive charge layers: a lower positive charge, a main negative charge, an upper positive charge, and a negative screening layer at the upper cloud boundary (e.g., Stolzenburg and Marshall, 2008, Fig. 2). Wu et al. (2012) "inferred that positive NBEs are produced between main negative charge layer and upper positive charge layer while negative NBEs are produced between upper positive charge layer and negative screening charge layer at the cloud top." Thus, in Wu et al. (2012), the positive NBEs occurred in a downward pointing electric field, E, while the negative NBEs occurred in an upward-pointing E. Negative NBEs also occur in the upward-pointing E found below the main negative charge (Rison et al., 2016; Bandara et al., 2019). However, Karunarathna et al. (2015) observed that positive NBEs "located above a thunderstorm's upper positive charge or near the top of anvil clouds may be initiated by small-scale charge regions with positive charge above negative charge (i.e., the opposite orientation of the large-scale storm charges…)." Herein we use NBE polarity to infer the vertical electric field that existed at the NBE's location in the radar context of the parent thunderstorm.

Surprisingly, only a few studies have presented evidence of NBE groups. Nag et al. (2010) studied 157 NBEs in Florida thunderstorms and identified three NBE groups; each group had a pair of NBEs that were separated by time intervals of 43, 66 and 181 ms and by horizontal distances of 16, 24 and 11 km, respectively. Although not presented as an NBE group, Rison et al. (2016) reported one pair of positive NBEs in a New Mexico thunderstorm that occurred within 2 ms and 500 m horizontally of each other; the first NBE in the pair initiated an IC flash. In a Florida thunderstorm Tilles et al. (2019) found a "cluster" of 10 NBEs that occurred in a six second interval; the ten NBEs were all located "between the main negative and upper positive charge regions" in the storm, were within 10 km horizontally of each other, and occurred with times between successive NBEs ranging from about 100 ms to 900 ms. Karunarathna et al. (2015) found that some relatively small regions in thunderstorms sometimes favor repeated occurrences of NBEs, thereby producing "recurrent sets" of NBEs. The horizontal spacing of the recurrent NBEs in their study was <600 m (and <1500 m in altitude), and the time between successive NBEs in recurrent sets ranged from 17 s to 353 s. Thus NBE groups have been recognized in a few previous studies, but have not been the main focus of these studies. Characteristics of occurrence and parameters of individual NBEs in NBE groups are the main focus of this study.

Most previous NBE studies have focused on high power NBEs, so relatively little is known about low power NBEs, especially those that did not initiate flashes. Rison et al. (2016) determined that the power of ten positive NBEs that initiated IC flashes ranged from 1 W to 274,000 W and that five negative NBEs that initiated CG flashes had powers ranging from 1 W to 630 W. Similarly, Bandara et al. (2019) found the powers of 33 negative NBEs that initiated CG flashes ranged from 1 W to 1290 W. Both Rison et al. (2016) and Bandara et al. (2019) found that the fast antenna data of low-power NBEs (< 25 W) were "more monopolar" rather than bipolar (Rison et al., 2016) (or equivalently, a single "hump" with the typical, small NBE overshoot peak lost in sensor noise (Bandara et al., 2019)). As we will show, low power NBEs are relatively common in NBE groups.

In this study we investigate groups of NBEs that occurred close to each other in time and nearby in space: within 10 km horizontally and within ±660 ms of the first large-amplitude NBE in the group. The goals of this study are to learn how common such groups are in Mississippi thunderstorms, to learn about the parameters of NBEs in groups (especially about small-amplitude NBEs), to locate the NBEs of each group in the storm's radar reflectivity structure, and to infer some details about the electric field structure(s) that produce multiple NBEs in relatively small volume(s) of a thunderstorm in relatively short times. In particular, we compare the NBE groups to one mechanism proposed to explain NBE initiation and development. Thus, studying NBE groups can provide new information about NBEs and about the thunderstorms that produce them.

2. Data and methodology

2.1. Instrumentation for detecting NBEs and other lightning events

The data used in this study were collected with a seven-station lightning sensor array extending over an area of about 60 km × 30 km (Marshall et al., 2019). Each station had four lightning sensors (Marshall et al., 2019): an *E*-change Fast Antenna or "FA" (10 ms decay time, bandwidth 16 Hz – 2.6 MHz), an E-change Slow Antenna or "SA" (1.0 s decay time, bandwidth 0.16 Hz – 2.6 MHz), an electric field time derivative sensor or "dE/dt" (bandwidth 0–2.5 MHz), and a VHF sensor or "Log-RF" (logarithmic power sensor with a bandwidth 186–192 MHz). Whenever the FA data exceeded a floating trigger threshold, all the sensors at the site collected 400 ms of data with 250 ms of pre-trigger data and 150 ms of post-trigger data. Triggered sensor data were digitized at 10 MegaSamples/s (MS/s) with a bit depth of 12, time-tagged to GPS, and recorded on site; the FA and SA data were averaged to 5 MS/s before recording.

The coordinates (x, y, z, t) of NBEs and other lightning events were obtained in one of two ways: from the FA data using the "PBFA" (Position By Fast Antenna) time-of-arrival technique described in Karunarathne et al. (2013) or from the dE/dt data using the "$\int$dE/dt" time-of-arrival technique described in Bandara et al. (2019). Both techniques require sensor data from at least five sites to determine an event location, and both use similar Monte Carlo schemes to estimate location errors. The origin of our coordinate system was defined to be at the "central" sensor site (also called the "EE" site). The fast antenna sensor at the EE site was more sensitive to distant lightning events than at other sites, so it often triggered on events that did not cause the other sensors to trigger and record data, as will be seen for one pair of NBEs below.

The Log-RF peak source power of NBEs was determined using the Friis transmission equation, as described in Bandara et al. (2019). We give Log-RF power (also called VHF power herein) in watts and, occasionally, in dBW (deciBels relative to 1 W) for comparison to other works. Power in dBW is equal to 10 $\log_{10}$(power in W), so 100 W = 20 dBW, 1000 W = 30 dBW, for example.

The FA *E*-change amplitudes of NBEs were range-normalized to 100

Table 1
Overview of 15 NBE groups.

Group #	Date (2016)	# NBEs	ΔT[a] (ms)	Δh[b] (km)	ΔR[c] (km)	ΔZ[d] (km)	$E_{1\text{-}2}$[e] (V/m)	$T_{1\text{-}2}$[f] (ms)	Group begin time (UT)	Group type
1	Aug. 5	2	170	4.06	4.08	0.4	130	170	20:56:09.6	Isolated
2	Aug. 5	2	99	6.12	6.13	−0.1	40	99	21:13:16.6	Not-Isolated
3	Aug. 5	2	147	1.84	2.20	1.1	1170	147	20:35:13.4	Isolated
4	Aug. 6	2	85	2.77	3.15	−1.5	370	85	19:35:06.1	Not-Isolated
5	Aug. 9	2	476	0.24	0.69	−0.6	51,500	476	23:42:54.2	Isolated
6	Aug. 26	2	21	5.4	5.5	−1.0	60	21	18:21:16.5	Isolated
7	Aug. 26	2	120	1.09	1.7	−1.3	2990	120	18:23:02.8	Isolated
8	Aug. 26	2	78	4.16	4.17	−0.3	120	78	18:38:15.5	Isolated
9	Aug. 26	2	10	3.98	4.50	2.1	130	10	19:03:25.3	Isolated
10	Aug. 26	3	52	6.02	7.42	−4.3	30	52	18:20:04.8	Not-Isolated
			177	4.37	5.13	−1.7	90	125		
11	Aug. 5	5	146	8.40	8.41	0.5	20	146	21:13:06.3	Isolated
			368	4.78	4.80	−0.4	50	222		
			444	3.03	3.12	0.8	210	76		
			446	2.81	2.82	0.2	200	2.4		
12	Aug. 5	2	31	4.87	5.17	−1.7	80	31	19:28:30.5	Isolated
13	Aug. 5	2	134	6.08	6.20	1.2	40	134	19:28:33.9	Isolated
14	Aug. 17	2	71	1.33	1.42	−0.5	3670	71	20:29:21.9	Not-Isolated
15	Aug. 6	3	94	4.32	8.60	−7.4	30	94	19:35:27.2	Not-Isolated
			148	4.97	5.05	−0.9	10	54		

[a] ΔT is time between NBE-1 and each of the other NBEs in the group, i.e., between NBE-1 & NBE-2, between NBE-1 & NBE-3, etc.
[b] Δh is the horizontal distance between NBE-1 and each of the other NBEs in the group.
[c] ΔR is the slant range between NBE-1 and each of the other NBEs in the group.
[d] ΔZ is the altitude difference between NBE-1 and each of the other NBEs in the group; values are positive when NBE-1 altitude is lower.
[e] $E_{1\text{-}2}$ is the magnitude of electric field at NBE-2 due to NBE-1 assuming the charge moment of NBE-1 was 1000C m, and similarly for successive NBE pairs (e.g., E_{23} at NBE-3 due to NBE-2 with charge moment of 1000C m).
[f] $T_{1\text{-}2}$ is time between NBE-1 and NBE-2, and similarly for successive NBE pairs (e.g., T_{23} is time between NBE-2 and NBE-3, etc.).

km, assuming the amplitude has a 1/R dependence, where R is the slant range from the NBE to the FA sensor (e.g., Marshall et al., 2014). We denote the normalized FA amplitudes as "E_{100km}" amplitudes.

2.2. Defining NBE groups

We define an NBE group as series of NBEs that all occurred within a 10 km horizontal radius and ± 660 ms from the first large-amplitude NBE in the group. These spatial and time parameters are the same as the isolation parameters used by Karunarathne et al. (2015) and Bandara et al. (2020) to categorize individual NBEs spatiotemporally. The ±660 ms time span was chosen in the earlier studies because it is the mean duration of IC flashes (Bils et al., 1988). Thus an individual NBE is isolated in time from other lightning flash events if there are no events within ±660 ms of the NBE, and we use the same time period for the temporal requirement for NBEs in groups. Note that compared to the recurrent NBE sets of Karunarathna et al. (2015), the NBEs in NBE groups defined herein occurred much closer together in time (< ±660 ms versus 17–373 s), but they could be much farther apart in horizontal distance (< 10 km versus <600 m).

To find NBE groups, we started with 319 positive NBEs that occurred in Mississippi thunderstorms during July and August of 2016. These NBEs were originally found by Bandara et al. (2020), who used Log-RF data to search for NBEs and FA data to determine NBE polarity. Each of the 319 NBEs had a Log-RF pulse with a peak amplitude greater than five times a threshold level chosen to "find only large Log-RF pulses"; the smallest powers in the 319 NBEs were > 100 W. The original search required that each positive NBE have an FA waveform with the typical bipolar NBE shape and that there would be data from at least five sensor sites so that the NBE could be located using either PBFA or ∫dE/dt (since the NBE's location was needed to calculate its VHF power). Thus each of the 319 positive NBEs had a substantial Log-RF pulse and had a coincident FA pulse with the characteristic bipolar waveform of a positive NBE. Then, for each positive NBE in the original collection of 319, we looked for any other NBEs of any polarity and any power that occurred within 10 km horizontally and within ±660 ms. Fifteen NBE groups were found and are described below.

2.3. Storm-relative locations of NBEs

We determined the location of each NBE in its thunderstorm environment, as indicated by the storm's radar reflectivity, using volumetric Plan Position Indicator (PPI) radar reflectivity scans from the Next Generation Weather Radars (NEXRAD) in Memphis, TN, and Columbus, MS, operated by the NOAA/National Weather Service. To investigate the storm radar structure coinciding with each NBE, the location given from $\int dE/dt$ or PBFA was overlaid on PPI radar reflectivity scans and on vertical cross sections of radar reflectivity data. Each radar volume is composed of 360° PPI azimuth scans at 14 elevation angles and takes 3.5 to 5 min to complete. The vertical cross sections are cut through the radar volume acquired in the 5 min time interval in which the NBE discharge happened (e.g., Karunarathna et al., 2015).

3. NBE groups

3.1. Overview

As described in Section 2.2, we looked for NBE groups within the 10 km and ± 660 ms of the 319 positive NBEs. We found 35 NBEs that occurred in 15 groups. Table 1 gives an overview of the 15 groups including a Group number, date and beginning time, number of NBEs per group, and relative time and position differences between pairs of NBEs in each group. There were 9 groups with two positive NBEs, 3 groups with one positive NBE and one negative NBE, one group of 3 positive NBEs, one group with two positive NBEs and one negative NBE, and one group of 5 positive NBEs.

As shown in Table 1, the horizontal separation, Δh, between the NBEs in a group (required to be <10 km) ranged from 0.18–8.4 km, and the time separation, ΔT, (required to be within 660 ms) ranged from 10 to 476 ms. For groups with only two NBEs, Δh is the magnitude of the difference in the horizontal locations of the first NBE to occur in the group (called NBE #1) and NBE #2; if there are more than two NBEs in the group, then the Δh values are between NBEs #1 and #2, then between NBEs #1 and #3, etc. The same scheme is also used for ΔT, ΔR, and ΔZ, where ΔR is the slant range between NBE pairs and ΔZ is the altitude difference between NBE pairs. For most groups the first NBE was

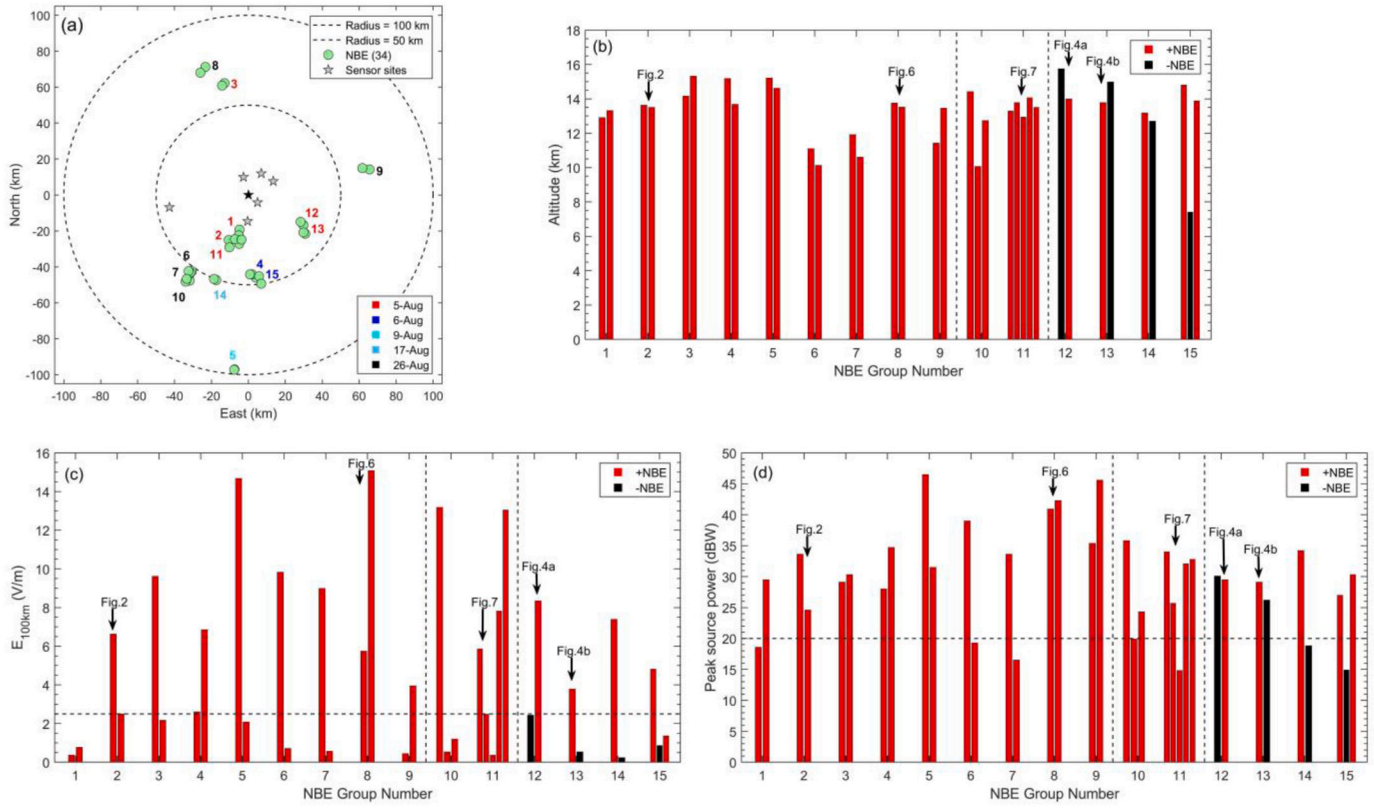

Fig. 1. (a) Plan positions of NBE groups relative to seven sensor sites marked by gray and black stars; the black star marks the "central site," which is the origin of the (x, y) coordinate system. NBEs marked with green circles. NBE Group numbers are color-coded by day in 2016. (b), (c), (d) Bar charts of NBE Groups; the horizontal axis gives the NBE Group number with one bar for each NBE in the Group: red bars for positive NBEs and black bars for negative NBEs. (b) NBE altitude. (c) NBE FA amplitude range-normalized to 100 km (E_{100km}). (d) NBE Log-RF (VHF) peak source power. (For interpretation of the references to colour in this figure legend, the reader is referred to the web version of this article.)

from the collection of 319 positive NBEs, but this was not always the case., Six groups included only NBEs from the collection of 319 NBEs. (We note that two of the groups had an additional positive NBE within the ±660 ms time limit; since these NBEs were not located, they were not included in the groups.)

Fig. 1(a) shows the plan position of the 15 NBE groups along with the sensor site locations. All 35 NBEs in the 15 groups occurred within a horizontal range of 100 km from the central sensor site with an average range and standard deviation of (49 ± 19 km) and a minimum range of 20 km. Table 2 gives details of each of the 35 NBEs in the groups, including FA range-normalized amplitude, VHF (Log-RF) power, (x, y, z) location relative to the central sensor site, χ^2 goodness of fit, and estimated errors of time and location. The more distant groups tended to have larger location errors; location errors were especially large for the most distant group, #5.

Although there were 25 days with data for nearby thunderstorms between July 9 and August 262,016 (usually with multiple thunderstorms per day), the NBE groups occurred in a total of just nine thunderstorms on only five separate days. As seen in Fig. 1(a), August 5, 6, 9, 17, and 26 had NBE groups in 3, 1, 1, 1, and 3 thunderstorms, respectively. Several of the groups occurred close in time and space. Groups 1, 2, and 11 occurred within 17 min in the same August 5th storm, with Groups 2 and 11 separated by only 10 s (shown in detail later). Groups 12 and 13 occurred about 1.5 h later in another August 5 storm and were separated by only 3 s (also shown in detail later). Groups 4 and 15 occurred in one thunderstorm on August 6 and were separated by only 21 s. On August 26 there was an outbreak of multiple thunderstorms in the area through several hours; five NBE groups were found in only three storms, with Groups 6, 7, and 10 occurring within a 3 min interval in one thunderstorm complex.

3.2. Altitudes of NBE groups

Fig. 1b shows the altitudes of the 35 NBEs in the 15 Groups, as given in Table 1. The altitudes of the 31 positive NBEs varied from 10.1–15.3 km with altitude mean and standard deviation of 13.3 ± 1.4 km, while the three high-altitude negative NBEs in Groups 12–14 occurred at 12.7, 15.0, and 15.7 km altitude. These 34 NBE altitudes are in reasonable agreement with many previous studies in that the altitude of positive NBEs are usually lower than typical, high-altitude, negative NBEs (e.g., Smith et al., 2004; Wu et al., 2014). The altitude of the 35th NBE is discussed next.

In Group 15 a low-altitude negative NBE occurred at 7.4 km and seemed to be a "precursor" NBE of a negative CG flash. Rison et al. (2016) defined a "precursor" as a positive NBE that occurs "seconds before an IC discharge initiates at the same location." The precursor examples in Rison et al. (2016) had powers of 12 and 146 W. The precursor negative NBE in Group 15 had a power of 31 W and occurred 25 ms before the first IB pulses of the CG flash. After the precursor NBE, the following IB pulses began 570 m below and 600 m horizontally from the precursor NBE location and developed downward, as typical for IB pulses of CG flashes (e.g., Stolzenburg et al., 2013). Although 25 ms is much shorter than the "seconds" described by Rison et al. (2016) between a precursor and an IC flash initiation, it (25 ms) is still much longer than the time (<1 ms) between an INBE and the first IB pulse in negative CG flash initiations by an INBE (Bandara et al., 2019), so we think the "precursor" designation is appropriate for this negative NBE. The altitude of the precursor NBE in Group 15 was in good agreement with the altitude range of 5.0–7.5 km for 18 low-altitude negative NBEs that initiated negative CG flashes (Bandara et al., 2019).

Thus, the altitudes of the 35 NBEs in Fig. 1b are in reasonable

Table 2
Parameters of individual NBEs in the 15 NBE groups[a].

Group #	NBE #	E_{100km} (V/m)	VHF power (W)	x (km)	y (km)	z Altitude (km)	χ^2	Δt (μs)	Δx (m)	Δy (m)	Δz (m)
1	1	0.4	72	−1.4	−21.6	12.9	2.4	0.6	93	149	195
1	2	0.8	883	−4.8	−19.3	13.3	1.3	0.6	82	144	213
2	1	6.6	2293	−10.7	−25.1	13.6	1.9	0.5	44	147	218
2	2	2.5	286	−4.6	−24.1	13.5	1.6	0.4	63	140	181
3	1	9.6	805	−13.0	62.2	14.2	4.7	1.2	60	385	616
3	2	2.2	1083	−14.3	60.9	15.3	4.5	1.1	57	352	535
4	1	2.6	632	4.0	−46.0	15.2	2.9	2.1	301	576	290
4	2	6.8	2924	1.9	−44.2	13.7	2.6	1.9	251	518	302
5	1	14.7	44,509	−7.6	−97.1	15.2	2.7	19.7	790	6161	2045
5	2	2.1	1406	−7.7	−97.2	14.6	2.9	18.7	777	5866	2357
6	1	9.8	7918	−30.6	−42.4	11.1	3.6	2.7	188	622	1079
6	2	0.7	85	−31.9	−47.7	10.1	3.7	2.9	212	724	1137
7	1	9.0	2297	−31.8	−44.1	11.9	4.1	2.7	204	644	948
7	2	0.6	45	−31.4	−43.1	10.6	3.8	2.4	186	580	979
8	1	5.7	12,246	−23.4	71.2	13.8	1.8	3.3	145	905	1483
8	2	15.1	17,174	−26.0	68.0	13.5	1.6	3.1	158	838	1499
9	1	0.4	3475	65.6	14.2	11.4	1.6	13.1	3774	919	1195
9	2	4.0	36,622	61.7	14.9	13.5	1.5	12.5	3538	939	1144
10	1	13.2	3783	−34.0	−48.2	14.4	4.7	2.0	172	484	610
10	2	0.5	98	−32.4	−42.4	10.1	3.8	1.6	143	400	654
10	3	1.2	268	−33.4	−46.7	12.7	4.3	1.9	160	477	588
11	1	5.9	2517	−5.2	−22.4	13.3	1.7	0.4	55	126	157
11	2	2.5	372	−10.3	−29.1	13.8	2.2	0.6	53	172	253
11	3	0.4	30	−5.0	−27.2	12.9	1.9	0.5	60	152	192
11	4	7.8	1606	−7.3	−24.6	14.1	2.2	0.5	53	141	183
11	5	13.0	1905	−3.8	−24.8	13.5	1.7	0.5	63	138	192
12	1	−2.4	1020	30.8	−21.6	15.7	2.0	2.5	654	479	377
12	2	8.3	884	29.8	−16.8	14.0	0.7	2.0	540	316	349
13	1	3.8	814	28.3	−15.0	13.8	0.5	1.8	470	269	359
13	2	−0.5	421	29.8	−20.8	15.0	0.6	2.3	615	438	351
14	1	7.4	2648	−17.4	−47.3	13.2	2.9	2.5	62	648	746
14	2	−0.2	76	−18.6	−46.7	12.7	2.9	2.4	47	631	741
15	1	4.8	496	5.7	−45.2	14.8	3.5	1.0	143	321	191
15	2	−0.9	31	6.9	−49.4	7.4	3.7	1.1	150	350	491
15	3	1.4	1070	0.9	−44.2	13.9	3.3	0.9	114	293	206

[a] x, y, z are NBE locations; Δt, Δx, Δy, and Δz are the estimated location errors; and χ^2 is the goodness of fit.

agreement with previous measurements. It is noteworthy that 28 of the 35 NBEs occurred at altitudes ≥12 km.

3.3. Range-normalized FA amplitudes of NBE groups

Fig. 1c shows the NBE FA amplitudes range-normalized to 100 km (E_{100km}) for the 15 groups. The E_{100km} values for the 31 positive NBE in the 15 groups ranged from 0.4 to 15.1 V/m with an arithmetic mean and standard deviation of (5.3 ± 4.6) V/m. Note that almost all groups had at least one NBE with $|E_{100km}| \leq 2.5$ V/m and these small-amplitude NBEs brought down the average. In the 15 groups there were 13 positive NBEs with $|E_{100km}| \leq 2.5$ V/m; these 13 NBEs had a mean and standard deviation of (1.2 ± 0.8) V/m, while the remaining 18 positive NBEs with $|E_{100km}| > 2.5$ Vm^{-1} had a mean and standard deviation of (8.2 ± 3.8) V/m, which is in good agreement with the values of (9.5 ± 3.6 Vm^{-1}) for 24 positive NBEs (Smith et al., 1999) and (11.0 ± 6.2 Vm^{-1}) for 226 positive NBEs (Karunarathne et al., 2015). In addition, Fig. 1c shows that E_{100km} values of the three typical, high altitude negative NBEs were −2.4, −0.5, and − 0.2 Vm^{-1}, and these values are relatively small compared to 22 high altitude (> 8 km) negative NBEs in Mississippi thunderstorms (Bandara et al., 2019), whose E_{100km} values ranged from −0.4 to −16.2 Vm^{-1} with mean and standard deviation of (−3.4 ± 4.1) Vm^{-1}. The precursor negative NBE in Group 15 had an E_{100km} value of −0.9 V/m, which is similar to the E_{100km} values of 18 low-altitude negative NBEs *initiating* negative CG flashes that had a range of −0.15 to −1.53 V/m with mean and standard deviation of −0.60 ± 0.39 V/m (Bandara et al., 2019). Based on the above data, we hypothesize that positive and negative NBEs with relatively small E_{100km} values are more common than previously recognized.

3.4. VHF powers of NBE groups

Fig. 1d shows the Log-RF peak source power in dBW for the 15 Groups, estimated using the Friis equation; the horizontal, dashed line indicates 100 W or 20 dBW. The source powers for 31 positive NBEs ranged from 30 to 44,500 W (14.8–46.5 dBW) with arithmetic mean of 4880 W (36.9 dBW) and a standard deviation of 10,300 W. Five of the 31 positive NBEs had powers <100 W (30, 45, 72, 85, 98 W). For comparison, Bandara et al. (2020) found, for 188 positive NBEs, that the average Log-RF power was 7900 W (39.0 dBW) with a standard deviation of 11,900 W and a range of 100–88,400 W. Three of the four negative NBEs occurred above 12 km altitude (Fig. 1b) and had peak radiated powers of 1020, 421, and 76 W; these NBEs were relatively small compared to the Log-RF powers of 22 high-altitude negative NBEs reported by Bandara et al. (2019), which had values ranging from "260 to 7420 W with an arithmetic mean of 1770 W (or 32.5 dBW)." The precursor negative NBE occurred at 7.4 km altitude with a power of 31 W. For comparison, Bandara et al. (2019) found that 18 negative NBEs that initiated CG flashes had powers of 9–1290 W with an average power of 230 W. Overall, most of the Log-RF powers of the NBEs in groups were in reasonable agreement with previous measurements, but finding Log-RF powers <100 W for 20% of the NBEs in the 15 groups supports the idea that there may be more low-power NBEs than previously recognized. One reason for this lack of recognition may be the fact that Le Vine (1980) emphasized that NBEs were the strongest sources of RF power from lightning, while another reason is simply that weak NBEs are more difficult to detect than strong NBEs.

4. Intra-group interactions with respect to NBE initiation

In this section we investigate NBE groups to see if earlier NBEs in a

Table 3
Expected EAS cosmic rays, expected NBEs, and Observed NBEs for NBE Groups.

Group #	T[a] (s)	Δh[b] (km)	A = πΔh[c] (km^2)	A_{NBEs}[d] (km^2)	Cosmic rays in A[e]	Cosmic rays in A_{NBEs}[f]	Expected NBEs[g]	N (Observed NBEs)[h]	Obseved/Expected[i] agree?
1	0.170	4.06	12.75	2.0	14.1	2.2	2.2	2	yes
2	0.099	6.12	19.23	2.0	12.4	1.3	1.3	2	maybe
3	0.147	1.84	5.78	2.0	5.5	1.9	1.9	2	yes
4	0.085	2.77	8.70	2.0	4.8	1.1	1.1	2	maybe
5	0.476	0.24	0.75	0.75[j]	2.3	2.3	2.3	2	yes[k]
6	0.021	5.4	16.96	2.0	2.3	0.27	0.27	2	no
7	0.120	1.09	3.42	2.0	2.7	1.6	1.6	2	yes
8	0.078	4.16	13.07	2.0	6.6	1.0	1.0	2	maybe
9	0.010	3.98	12.50	2.0	0.8	0.13	0.13	2	no
10	0.177	6.02	18.91	3.0	21.8	3.45	3.45	3	yes
11	0.446	8.40	26.39	5.0	76.5	14.5	14.5	5	Yes[k]
12	0.031	4.87	15.30	2.0	3.1	0.4	0.4	2	no
13	0.134	6.08	19.10	2.0	16.6	1.7	1.7	2	yes
14	0.071	1.33	4.18	2.0	1.9	0.9	0.9	2	maybe
15	0.148	4.97	15.61	3.0	15.0	2.9	2.9	3	yes

[a] Time in Eq. (1), determined from Table 1.
[b] Δh is greatest horizontal distance between an NBE pair in the NBE group, determined from Table 1.
[c] Area A equals area of circle with diameter Δh.
[d] A_{NBEs} = area of observed NBEs in NBE group, assuming 1 km^2 per NBE.
[e] Calculated using Eq. (1) using A and T.
[f] Calculated using Eq. (1) using A_{NBEs} and T.
[g] Equals Cosmic rays in A_{NBEs}.
[h] N equals number of NBEs in NBE group.
[i] "Yes" if Expected NBEs rounded to integer = N (or more than N, see text for reason),; "maybe" if Expected NBEs rounded to integer is (N-1); "no" if Expected NBEs <0.5.
[j] Used A_{NBEs} = 0.75 km^2 since Group 5 apparently had two NBEs in the same volume with horizontal area of 0.75 km^2.
[k] Different reason for "yes"; see text for details.

group help initiate subsequent NBEs in the group. For NBE-1 to help initiate NBE-2, the electric field, $E_{1\text{-}2}$, due to NBE-1 at the location of NBE-2 should be relatively large, large enough when added to the thunderstorm electric field to initiate NBE-2. We estimated what $E_{1\text{-}2}$ "large" means by considering the thunderstorm electric field E_{th} needed to initiate an NBE, namely 3 MV/(m·atm) as suggested by Kostinskiy et al. (2020a). At the altitudes of the NBEs in groups, the E_{th} would be smaller by a factor of the air pressure at NBE altitude divided by the pressure at z = 0 km. The NBE altitudes in the NBE groups ranged from 7.4 km to 15.7 km (Table 2). For representative altitudes of 10.0, 13.0, and 15.0 km, the pressure-scaled E_{th} is 910, 640, and 500 kV/m, respectively. Choosing the "large" value of $E_{1\text{-}2}$ to be 10% of E_{th} gives $E_{1\text{-}2}$ values of 91, 64, and 50 kV/m, respectively, at altitudes of 10.0, 13.0, and 15.0 km.

We calculated $E_{1\text{-}2}$ as follows for the 12 NBE groups with two NBEs. Knowing the slant range between NBE-1 and NBE-2 (ΔR in Table 1), we calculated $E_{1\text{-}2}$ assuming NBE-1 had a vertical charge moment of 1000C m; $E_{1\text{-}2}$ varies inversely as $(\Delta R)^3$. The 1000C m dipole moment value was based on the charge moment average and standard deviation of (1090 ± 360) C m for ten NBEs detected at close range by Karunarathne et al. (2016). For NBE groups with 3 NBEs, we calculated $E_{1\text{-}2}$ as just described; then for NBE-3 we calculated $E_{1\text{-}3}$ and $E_{2\text{-}3}$ by assuming that NBE-1 and NBE-2 both had a charge moments of 1000C m, and, for simplicity, added the magnitudes of $E_{1\text{-}3}$ and $E_{2\text{-}3}$ together to estimate their possible influence on initiating the third NBE. The group of five NBEs was handled similarly, but with the additions of the first three NBEs influencing the 4th NBE and the first four NBEs influencing the 5th NBE.

With one possible exception, all of the electric fields of an NBE at the location of subsequent NBEs of a group (the $E_{1\text{-}2}$ values in Table 1) were less than 4 kV/m, so early NBEs were not significantly helping to initiate subsequent NBEs in a group. The possible exception was the pair of NBEs in Group 5; these NBEs were quite close together (ΔR = 0.69 km) and occurred at 15.2 and 14.6 km altitude (Table 2), so their $E_{1\text{-}2}$ value of 51.5 kV/m was "large" compared to 50 kV/m defined for 15 km altitude. However, we should note that this NBE group had by far the largest location uncertainties of any NBE group, because it was the farthest group from the sensor array (~100 km, see Fig. 1a). If possible errors in these locations led to the actual separation of NBEs in Group 5 of just 25% greater distance, then $E_{1\text{-}2}$ would have been reduced to 26 kV/m, well lower than the "large" threshold for 15 km altitude. Thus, we conclude that none or almost none of the earlier NBEs in NBE groups were involved in initiating the later NBEs in each NBE group. This means that all or almost all of the NBEs in the NBE groups initiated independently in a large-amplitude, local electric field.

5. Comparing NBE groups in context with an NBE initiation mechanism

In the previous section we found that most or all NBEs in NBE groups are initiated independently of each other. In this section, we check to see if a recently proposed NBE mechanism fits with available data on NBE groups.

Based on VHF interferometer measurements, Rison et al. (2016) stated that an NBE does not "*produce a conducting channel, but instead appears to consist of a volumetrically distributed system of positive streamers*" with horizontal scales of 100–150 m and vertical scale of 500–600 m. Two different mechanisms for producing the system of positive streamers have been suggested. We call the first of these the "hydrometeor-corona" mechanism. Rison et al. (2016) stated that the positive streamers "*would be initiated by corona from ice crystals or liquid hydrometeors,*" and several NBE models based on this hypothesis have been constructed (e.g., Babich et al., 2016; Attanasio et al., 2019). However, Rutjes et al. (2019) have questioned the hydrometeor-corona mechanism because under normal conditions there are essentially no free thermal electrons inside thunderclouds to start the positive streamers. Rutjes et al. (2019) suggested that an extensive air shower (EAS) due to a high-energy cosmic ray might provide free thermal electrons for the hydrometeor-corona mechanism; however, almost all of the free electrons are located less than a meter from the EAS core, making it difficult to explain the observed 100–150 m horizontal extent of NBEs, as noted by Rutjes et al. (2019). Rutjes et al. (2019) suggested that an EAS with an

especially large electric field and an especially high density of appropriately-shaped hydrometeors might cause the positive streamers of an NBE. Overall, it seems there remain some uncertainties concerning the hydrometeor-corona mechanism.

The second NBE mechanism is the "turbulence-EAS/RREA" (EAS-RREA means an EAS followed by a relativistic runaway electron avalanche or RREA), proposed by Kostinskiy et al. (2020a) as part of their lightning initiation mechanism. Kostinskiy et al. (2020a) hypothesized, based on data from Marshall et al. (2019) and others, that NBEs and much weaker VHF events can initiate lightning flashes, and they suggested that "*initiation occurs in a region of ~1 km^{3}with average electric field E>0.3 MV/(m•atm), which contains, because of turbulence, numerous small 'E_{th}-volumes' of ~ 10^{-4}–10^{-3} m^{3}with E ≥ 3 MV/(m•atm)*." The turbulence-EAS/RREA mechanism states that each NBE is caused by "*a group of relativistic runaway electron avalanche particles (where the initial electrons are secondary particles of an extensive air shower) passing through many E_{th}-volumes, thereby causing the nearly simultaneous launching of many positive streamer flashes.*" In this mechanism, the free thermal electrons (needed to start the positive streamers) are produced primarily by relativistic electrons and positrons of both the EAS and the RREA, while turbulence of charged cloud particles and charged hydrometeors produces the small scale regions with E ≥ 3 MV/(m•atm). As discussed in Kostinskiy et al. (2020b), the RREA provides lateral spreading of relativistic electrons/positrons of about 200 m, which is important in making an NBE with horizontal dimensions of 100–150 m. (In passing we note that an EAS-RREA might also offer a way to provide sufficient free thermal electrons with reasonable lateral extents for the hydrometeor-corona mechanism.)

The NBE groups can be used to test the turbulence-EAS/RREA mechanism, in particular to see if there were a sufficient number of EASs to cause the NBEs in each group. Rutjes et al. (2019) showed that the most probable energies for EASs causing NBEs were in the range 10^{15}–10^{17} eV, and they developed an equation that gives the average number, k, of cosmic rays in this range that would pass through a horizontal area A (in km^2) during a time T (in seconds):

$$k = 6.5 \bullet A \bullet T \quad (1)$$

It is important to remember that the cosmic rays are really random events in both time and space, so k just gives an estimate of the possible number of cosmic rays in A and T.

Table 3 lists the NBE groups and their A and T values. For each NBE group we use the time between the first and last NBEs (from Table 1) for T in Eq. (1). Since we have only one horizontal distance, Δh, for the groups with only two NBEs, we determine A in Eq. (1) as the circular area π•Δh. For NBE groups with multiple Δh's, we choose the longest Δh; e.g., for NBE group 11 Δh = 8.40 km and A = 26.4 km^2. Accordingly, Eq. (1) is used to determine, for each NBE group, the number of EAS cosmic rays that pass through A in time T. Table 3 also shows the total area, A_{NBEs}, associated with the NBEs of each group. If N is the number of NBEs in an NBE group, then $A_{NBEs} = N \bullet 1$ km^2, since 1 km^2 is the area of each NBE based on the ~1 km^3 volume which contains the many E_{th}-volumes needed to start the positive streamers (Kostinskiy et al., 2020a).

Now consider NBE group 1 with two positive NBEs that occurred 0.170 s and 4.06 km apart. The area A is 12.75 km^2, and the number of EAS cosmic rays that passed through A during 0.170 s was 14.1. The fact that there were only 2 NBEs and not 14 NBEs indicates that the whole volume associated with the 12.75 km^2 area did not have E ≥ 3 MV/(m•atm) nor does the whole volume contain a large number of very small E_{th}-volumes with E ≥ 3 MV/(m•atm). The same fact also indicates that there were at least 2 separate regions containing E_{th}-volumes with E ≥ 3 MV/(m•atm). Including NBE group 1, nine of the 15 NBE groups had substantially more EAS cosmic rays than NBEs, so the whole volume associated with each of these groups did not have E ≥ 3 MV/(m•atm) throughout, but instead had localized regions with E ≥ 3 MV/(m•atm) in which the NBEs occurred.

Continuing with NBE group 1: since $N = 2$, $A_{NBEs} = 2.0$ km^2. (A_{NBEs} is part of A.) The number of EAS cosmic rays passing through A_{NBEs} in time T, using Eq. (1), is 2.2 cosmic rays. Further, since these cosmic rays should cause NBEs, then "Expected NBEs" is 2.2 NBEs, which agrees nicely with the observation of 2 NBEs. These values are shown in Table 3. Cases with agreement in number between *NBEs expected* from the EAS cosmic rays and the *NBEs observed* are marked with "yes" in the rightmost column of Table 3. Eight of the 15 NBE groups had their expected number of NBEs (rounded to the nearest integer) equal to the observed number of NBEs in the group, so data for these eight NBE groups support the turbulence-EAS/RREA mechanism. Two of the NBE groups are marked "yes" (NBE groups 5 and 11) despite using different reasoning, and we discuss these groups next.

We marked NBE group 11 as "yes" in Table 3 even though there were 14.5 expected NBEs and only 5 NBEs detected because of the following reasoning: Suppose there were only five volumes of 1 km^3 ready to develop an NBE, then the first EAS cosmic ray passing through each of these five volumes would cause an NBE, but subsequent cosmic rays passing through these five volumes probably would not be able to cause additional NBEs.

We marked NBE group 5 as "yes" in Table 3, but its area A was only 0.75 km^2. Recall that Δh might have large error because of larger than typical location uncertainties in this case. However, let us assume that Δh = 0.24 km and A = 0.75 km^2 and further assume that the 2 NBEs of Group 5 both occurred in a volume with A = 0.75 km^2 separated in time by 0.476 s. Then both A and A_{NBEs} would be 0.75 km^2, and the number of EAS cosmic rays through both areas (from Eq. (1)) is 2.3, leading to 2.3 NBEs expected, in agreement with the 2 NBEs observed. It is difficult to understand how one small NBE volume could produce two NBEs in less than half a second, unless the first does not fully discharge the volume and leaves behind sufficient high-field region for another to initiate. We note that NBE-1 of Group 5 was strong with $E_{100km} = 14.7$ V/m and VHF power = 44,509 W, and NBE-2 was much weaker with $E_{100km} = 2.1$ V/m and VHF power = 1406 W.

Additional support for the turbulence-EAS/RREA mechanism is found in the four NBE groups marked with "maybe" in Table 3, indicating that the expected number of NBEs (rounded to the nearest integer) was one less than the observed number of NBEs. The "maybe" designation recognizes the fact that we have simply used the lower limits of T and of A based on the observations, without considering any extended time over which the NBEs might occur or any possible errors in locations.

Only 3 NBE groups have the number of expected NBEs much smaller than the number of observed NBEs, which does not seem to fit with the turbulence-EAS/RREA mechanism. However, the time intervals of these three NBE groups were the shortest of the 15 NBE groups (T of only 10, 21, and 31 ms), which contributes to the relative lack of expected cosmic rays and expected NBEs. For each of these three NBE groups to fit with the turbulence-EAS/RREA mechanism, a statistical fluctuation (an increase) in the number of EAS cosmic rays would have to have occurred, which is not impossible.

This test of the turbulence-EAS/RREA mechanism of Kostinskiy et al. (2020a) was made possible because 2, 3, or 5 NBEs occurred at known locations with horizontal separations <9 km and with time separations <500 ms (Tables 1 and 2). The test minimized the number of possible EAS cosmic rays "available" to cause the NBEs of an NBE group by limiting both A and T in Eq. (1), with A proportional to the horizontal distance between the observed NBEs and T equal to the time between the first and last NBEs. Despite this minimization, we have shown that for twelve of the 15 NBE groups there was good agreement between the expected number of NBEs and observed number of NBEs.

6. Spatiotemporal relation of NBE groups with other lightning events

Similar to the spatiotemporal definition of an individual NBE, we defined each NBE group as an Isolated group, a Not-Isolated group, or an

Table 4
Spatiotemporal category of NBEs groups[a].

NBE group type	Number of groups	Isolated	Not isolated	INBE
Two Positive NBEs	9	7	2	0
Three Positive NBEs	1	0	1	0
Five Positive NBEs	1	1	0	0
One Positive NBE and One Negative NBE	3	2	1	0
One Negative and Two Positive NBEs	1	0	1	0

[a] Spatiotemporal category relative to other lightning events (not NBEs).

Initiator group, based on the locations of non-NBE lightning events within a 10 km radius and a time interval of ±660 ms from the first NBE of the group. Recall that the locations of NBEs and non-NBE events were determined with the PBFA or ∫dE/dt methods; each location required triggered data from the FA or dE/dt sensors from at least five of the seven sensor sites. It is important to note that we base the spatiotemporal classification of NBE groups on the available location data, which might not include locations of weak lightning events.

Table 4 shows the spatiotemporal categories of the 15 NBE groups. None of the NBEs in the 15 NBE groups initiated a CG or an IC lightning flash. Ten NBE groups were Isolated from other lightning events, and five NBE groups were Not-Isolated. In the following subsections we give details and examples of spatiotemporal NBE groups, including using radar data to show where they occurred in their parent thundercloud.

6.1. INBE groups

In defining an NBE group as an INBE group, one of the NBEs in the group would have initiated either an IC flash or a CG flash. Based on the INBE requirements discussed above, we required that the IB pulses of an initiated IC or CG flash must begin within 10 ms (IC) or 1 ms (CG) of an

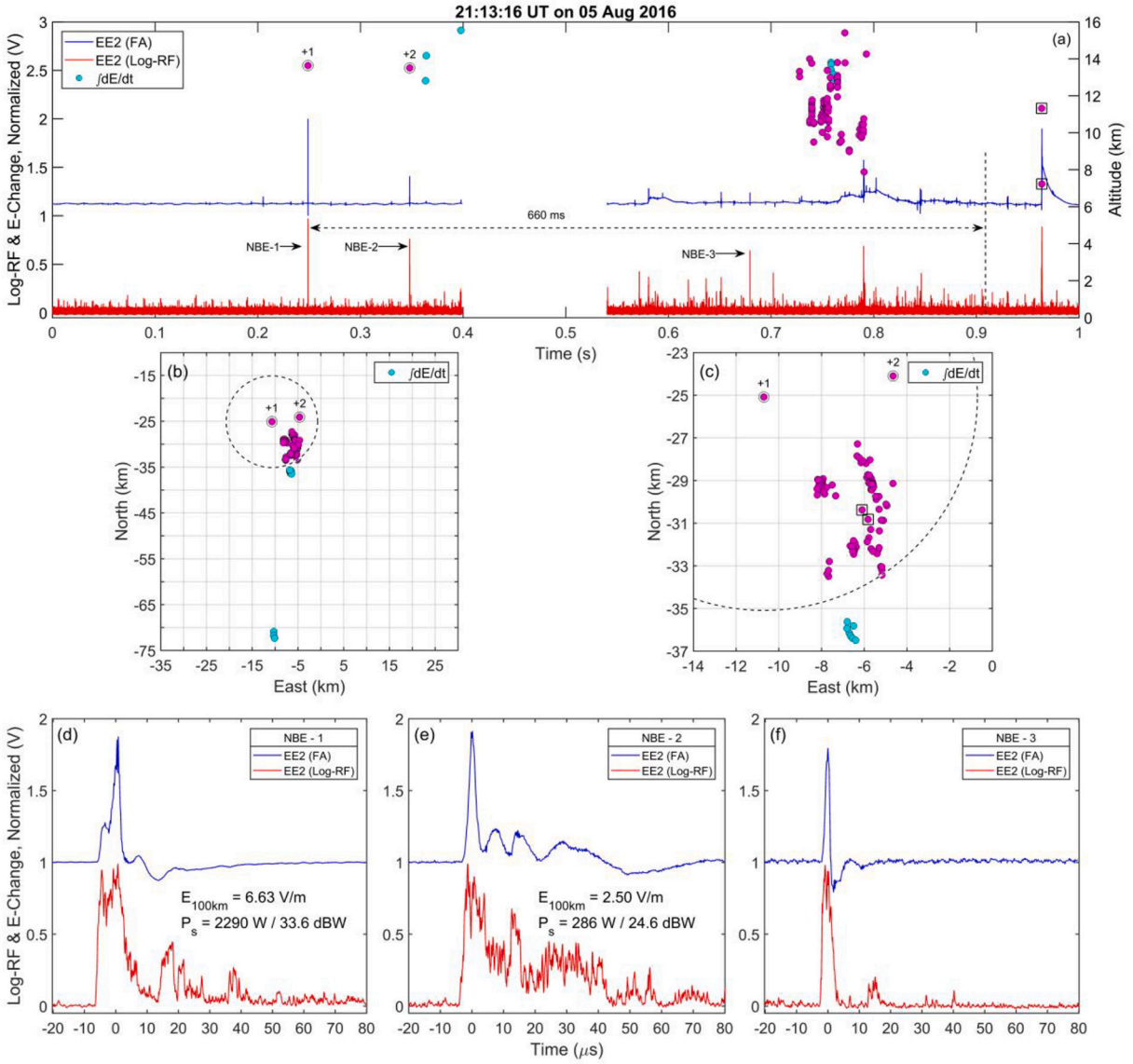

Fig. 2. Example of a Not-Isolated NBE Group with two positive NBEs (Group 2). A third positive, unlocated NBE (NBE-3) occurred about 400 μs after NBE 1. (a) Overview showing 1.0 s of triggered FA data (blue) and Log-RF data (red) as normalized voltages (left axis). Colored dots give altitudes (right axis) of locatable FA pulses (determined using ∫*dE/dt*) with events <10 km from NBE-1 colored magenta and events >10 km from NBE-1 colored cyan. (b) Plan view of lightning locations shown in (a); the dashed circle shows 10 km range from NBE-1. The three southern-most cyan events occurred <50 ms after NBE-2. (c) Expanded plan view of lightning events near NBE-1. The seven southern-most cyan events occurred ~400 ms after NBE-2. (d), (e), (f) Expanded views (100 μs) of NBEs shown in (a). (For interpretation of the references to colour in this figure legend, the reader is referred to the web version of this article.)

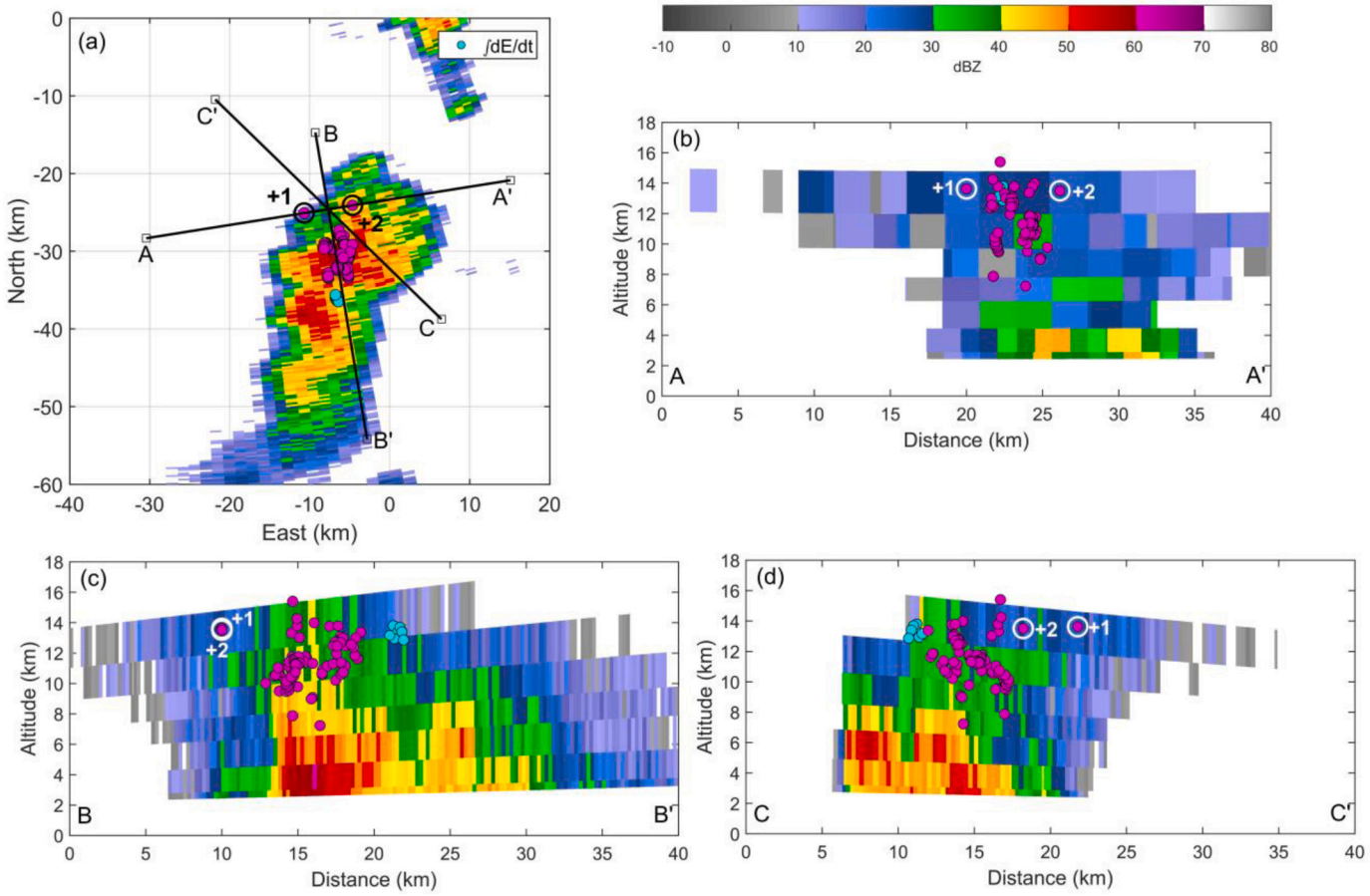

Fig. 3. Radar reflectivity along with NBEs and IC lightning events shown in Fig. 2(c). (a) NBEs (numbered black circles) and IC lightning events superimposed on PPI radar scan (3.4° elevation angle). Lines A–A′, B–B′, and C–C′ indicate the plan view locations of vertical radar cross-sections; event locations are projected perpendicularly onto each vertical cross-section while retaining their altitudes. (b) Vertical radar cross-section A–A', which passes through NBE-1 and NBE-2. (c) Vertical radar cross-section B–B′, which is perpendicular to A–A' and passes midway between NBE-1 and NBE-2. (d) Vertical radar along cross-section C–C′.

NBE in the group (e.g., Wu et al., 2014; Bandara et al., 2019).

Triggered data exist for all of the NBEs in each group, though for a few groups there are gaps in the triggered data between NBEs separated in time by more than 150 ms. (An example of a gap in triggered data is shown below.) The triggered data show that in no case was an NBE followed by a series of IB pulses within 10 ms. Thus, based on the above definitions, none of the 35 NBEs in the 15 NBE groups initiated a flash, so none of the 15 NBE groups were INBE groups. Importantly, this means that the groups of NBEs were not a series of attempted flash initiations that eventually started a flash. However, the negative NBE in Group 15 was a precursor of a CG flash, so it may have helped initiate that CG flash.

6.2. Not-Isolated NBE groups

"Not-Isolated" NBE groups are of interest because the thunderstorm has to provide the electrical conditions to initiate the NBEs and to initiate, without NBEs in these cases, the nearby IC or CG flash. Five of the 15 NBE groups were Not-Isolated. Fig. 2 shows an example of a Not-Isolated NBE group with two positive NBEs (Group 2 in Fig. 1) followed by an IC flash.

Fig. 2a displays 1.0 s of FA and Log-RF data (from the EE site) along with altitudes of located lightning events. Note the gap in triggered data. The first 400 ms of Fig. 2a represents the data from one triggering event (NBE-1) with 250 ms of pre-trigger and 150 ms of post-trigger data; NBE-2 occurred during the 150 ms of post-trigger data. Six sensors triggered on NBE-1 at time 0.25 s in Fig. 2a. The 150 ms of post-trigger data show that neither NBE initiated a lightning flash (since no IB pulses occurred within 10 ms of either NBE). The next triggering event at the EE sensor (the central site, shown in Fig. 1a) occurred roughly 540 ms after NBE-1 at about 0.79 s in Fig. 2a, but only two other sensor sites triggered, so no locations were possible. The third triggering event at the EE sensor occurred at about 0.97 s; four other sensors also triggered, so event locations began 250 ms before 0.97 s, as shown. This explains why NBE-3 was not located and why lightning pulses between 0.53 and 0.72 s in Fig. 2a were not located. The locations after 0.72 s were due to lightning pulses of an IC flash that was already in progress at time 0.72 s in Fig. 2a. It is not possible to determine when or where this IC flash began, but the data in Fig. 2a indicate that the IC flash initiated >150 ms after NBE-1 and < 480 ms after NBE-1.

Fig. 2b shows a plan view of lightning locations from Fig. 2a; the dashed circle is 10 km range from NBE-1. Most of the located events occurred close to NBE-1 and NBE-2, but the three southern-most events that occurred <50 ms after NBE-2 were located about 50 km south of the NBEs. These three events were probably part of a distant IC flash. Furthermore, these three events probably were not influenced by the Group 2 NBEs and probably did not influence the later IC flash near the NBEs. Fig. 2c shows an expanded view of Fig. 2b. The time and the horizontal separations between NBE-1 and NBE-2 were 99 ms and 6.1 km and $E_{1\text{-}2}$ was only 40 V/m (Table 1), so it seems unlikely that NBE-2 was initiated by NBE-1. The located IC flash events began about 480 ms after NBE-1 and 4.9 km horizontally from NBE-1 and 3.8 km horizontally from NBE-2. Overall, we can state that Group 2 was "Not-Isolated" since an IC flash occurred <10 km horizontally from NBE-1 and < 660 ms after NBE-1. Thus two NBEs and possibly one IC flash initiated within 10 km and 660 ms of each other. Considering the initiation mechanism of Kostinskiy et al. (2020a) and the discussion of NBE initiations in Section 5, we speculate that all three initiations were probably independent, occurred in three small regions with very large electric fields, and were initiated by three independent EAS-RREAs.

Each NBE in Fig. 2a had a substantial FA pulse coincident with a substantial Log-RF pulse. Fig. 2d, e, and f show expanded views (100 μs) of the three positive NBEs, including, for the located NBEs, the range normalized FA amplitude (E_{100km}) and the VHF peak power. NBE-1 had E_{100km} and VHF power values (6.6 V/m and 2300 W) close to the average values for the NBE groups (5.3 V/m and 4880 W, Sections 3.3 and 3.4), but NBE-2 had much smaller values (2.5 V/m, 290 W).

Fig. 3 shows NBE Group 2 overlaid on radar reflectivity data. The positive NBEs occurred ~30 km from the central sensor site and had location errors of dx ≤ 70 m, dy ≤150 m, and dz. ≤ 220 m (Table 2). Fig. 3a shows horizontal locations of the NBEs and the IC flash events of Fig. 2 superimposed on a PPI radar reflectivity scan along with lines indicating the locations of three vertical radar cross sections. Vertical radar cross sections are shown in Fig. 3b, c, and d, respectively. The radar cloud top was ~14 km in the vicinity of NBE-1 and NBE-2 (see Fig. 3b which passes through these two NBEs); NBE-1 and NBE-2 occurred in reflectivities of about 25 dBZ at altitudes of 13.6, and 13.5 km, respectively. The IC flash developed primarily in and above the high reflectivity storm core at altitudes between 8 and 16 km (Fig. 3c, which is approximately along the storm's direction of slow southward motion, toward B′). Notably, the positive NBEs of Group 2 occurred in the upper part of the down-shear anvil cloud, about 5 km horizontally away from (behind) the core and the IC flash locations (Fig. 3c, d). In Fig. 3c the 40 dBZ echo extended up to altitudes of at least ~13.5 km and maybe as high as 14.5 km (Fig. 3d), indicating that the storm had a very vigorous updraft, sufficient to loft relatively large hydrometeors to high levels. We speculate that the occurrence of numerous NBEs in this NBE group was related to the fact that this storm was dynamically intense at the time.

The occurrence of positive NBE-1 and positive NBE-2 in the upper part of the thunderstorm anvil is difficult to understand because positive NBEs require a downward-pointing electric field for initiation, while the large-scale electric field at their locations could be expected to be upward-pointing for the following reason. Thunderstorm anvil clouds typically carry positive charge from the storm core as an approximately horizontal charge layer moving away from the storm core, and negative screening charge layers develop at the upper and lower anvil boundaries (e.g., Marshall et al., 1989). Based on their positions above the highest reflectivity in the anvil (Fig. 3c and d), NBE-1 and NBE-2 may have occurred above the positive charge in the anvil where E would be upward pointing, not downward pointing. Karunarathna et al. (2015) found several positive NBEs in Florida thunderstorms in similar locations in anvil clouds. Karunarathna et al. (2015) hypothesized that the necessary downward pointing electric field needed to make a positive NBE in an anvil might be caused by either (i) small-scale turbulent motions acting on the large-scale charge layers, or (ii) anvil lightning followed by new screening layer formation. Based on the locations of NBE-1 and NBE-2, we hypothesize that the downward-pointing E needed for these NBEs was likely caused by one of the mechanisms suggested by Karunarathna et al. (2015). However, the electrical structure of anvils clouds is sometimes more complicated than found by Marshall et al. (1989). Byrne et al. (1989) and Stolzenburg et al. (2010) both found positive and negative charge layers at upper levels inside anvil clouds in addition to screening charge layers; anvil clouds with these more complicated structures could produce NBEs of either polarity, in relatively close proximity.

Overall, this example of a Not-Isolated group of two positive NBEs indicates that the electric field in thunderstorm anvil cloud was more complicated than the relatively simplistic charge structure described in Marshall et al. (1989). There were two locations in the thunderstorm anvil, separated by 99 ms and 6.1 km, with electric fields of unexpected polarity for the anvil (downward pointing) that were large enough to initiate two positive NBEs, while <480 ms after the first NBE and probably about 5 km horizontally from it, a IC flash occurred in the storm core, indicating that a downward pointing E also existed at the IC flash location, as expected for the four-charge thunderstorm updraft charge structure shown in Stolzenburg and Marshall (2008).

The other four Not-Isolated NBE groups (#4, 10, 14, and 15) can be described briefly as follows. The first NBE in NBE Group 4 (with two positive NBEs) occurred 411 ms after and 5.6 km horizontally from the last return stroke in a three-stroke negative CG flash. Most of the CG flash events occurred below 7.0 km (maximum altitude of 8.4 km) while

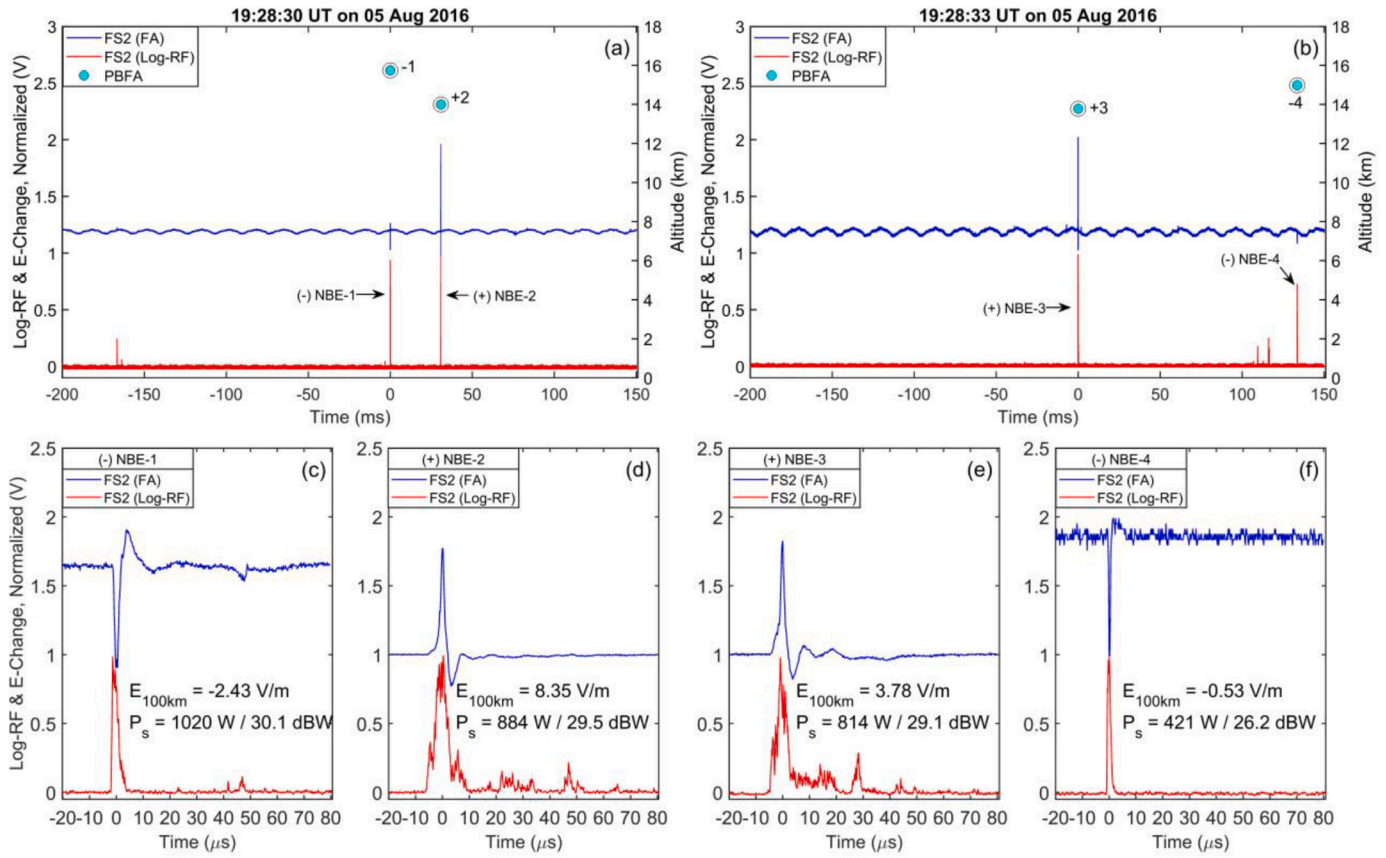

Fig. 4. Similar to Fig. 2, showing two Isolated NBE groups, each with one positive NBE and one negative NBE. NBE altitudes were determined using PBFA. (a), (b) Overviews (350 ms) of Groups 12 and 13, respectively, showing FA and Log-RF data. (c), (d) Expanded views (100 μs) FA and Log-RF waveforms, respectively, of Group 12 NBEs. (e), (f) Expanded views (100 μs) FA and Log-RF waveforms, respectively, of Group 13 NBEs.

the two positive NBEs occurred at 15.2 and 13.7 km altitude. Relative to radar, NBE-1 occurred above the reflectivity core near the upper echo boundary, and NBE-2 occurred high in the storm anvil. Thus two NBEs and one CG flash all initiated apparently independently of each other but within 10 km and 660 ms of each other, meaning that there were likely three locations with the very large electric field conditions needed for the initiations.

NBE Group 10 (three positive NBEs) was close in space and time to a three-stroke negative CG flash. The first two NBEs of Group 10 occurred, respectively, 202.0 ms and 150.0 ms before, and 2.5 km and 5.8 km horizontally from, the first return stroke. NBE-1 was located above the reflectivity core at 14.4 km altitude and NBE-2 was in the core at 10.1 km altitude. NBE-3 also occurred above the core at 12.7 km altitude, 25 ms before and 3.2 km from the first return stroke. As with most other groups, the NBEs in Group 10 occurred at higher altitudes than the CG flash events, which occurred mainly below 8.0 km. The third NBE in Group 10 was notable for occurring as the second event in the negative CG flash, only 39 μs after the initiating event of the flash, despite being a positive NBE (rather than a negative NBE, as those which precede some CG flashes). Since the three NBEs and one CG flash all initiated apparently independently of each other, four locations existed with the very large electric field conditions needed for these initiations.

NBE Group 14 (one positive NBE and one negative NBE) apparently occurred during a weak IC flash; only two pulses from the IC flash had sufficient amplitudes to be located. The NBEs of Group 14 occurred at 13.2 and 12.7 km altitude, close together and above a sheared reflectivity core. The two located IB pulses occurred at 12.7 and 12.0 km altitude; all four events occurred within a 2 km × 3 km horizontal area. Thus it is clear that the NBE Group 14 was Not-Isolated, but there is too little information about the IC flash to draw additional conclusions.

The first NBE (positive) in NBE Group 15 (two positive NBEs and one negative NBE) occurred 22 s after NBE Group 4 and was not isolated from a single return stroke, negative CG flash; the first NBE occurred 141 ms before and 4.5 km horizontally from the return stroke at an altitude of 14.8 km. The second NBE (negative) occurred 48 ms before the return stroke and 1.7 km horizontally from the return stroke at an altitude of 7.4 km, low in the reflectivity core. This negative NBE was the precursor NBE discussed earlier (in Section 3.2); it occurred about 25 ms before, 570 m above, and 600 m horizontally from the first few initial breakdown pulses of the CG flash, so it may have influenced the CG flash initiation. However, the negative NBE was not an INBE because the 25 ms between the NBE and the first initial breakdown pulse was longer than our definition (< 1 ms) for an INBE of a CG flash allows. The third NBE (positive) occurred 5.8 ms after and 9.4 km horizontally displaced from the return stroke at an altitude of 13.9 km. As in the case of NBE Group 4, the positive NBEs in Group 15 occurred at relatively high altitudes (14.8 km and 13.9 km) with NBE-1 above the reflectivity core and NBE-3 high in the anvil. Because NBE-2 seemed to be a precursor of the CG flash initiation, we can state that the initiations of three NBEs and one CG flash indicates that three (or perhaps four) separate locations existed at the time of Group 15 with the very large electric field conditions needed for the initiations.

Overall, the five Not-Isolated NBE Groups occurred near (in time and space) to typical IC flashes (two NBE Groups) or typical negative CG flashes (three NBE Groups), but the NBEs did not initiate these flashes nor did the NBEs seem to be initiated by the flashes. The altitudes of the NBEs in the Not-Isolated NBE Groups had an average and standard deviation of (12.9 ± 2.2 km) with values spanning 7.4–15.2 km. The positive NBEs in the three NBE groups close to CG flashes occurred at much higher altitudes than the CG flash events, and were horizontally

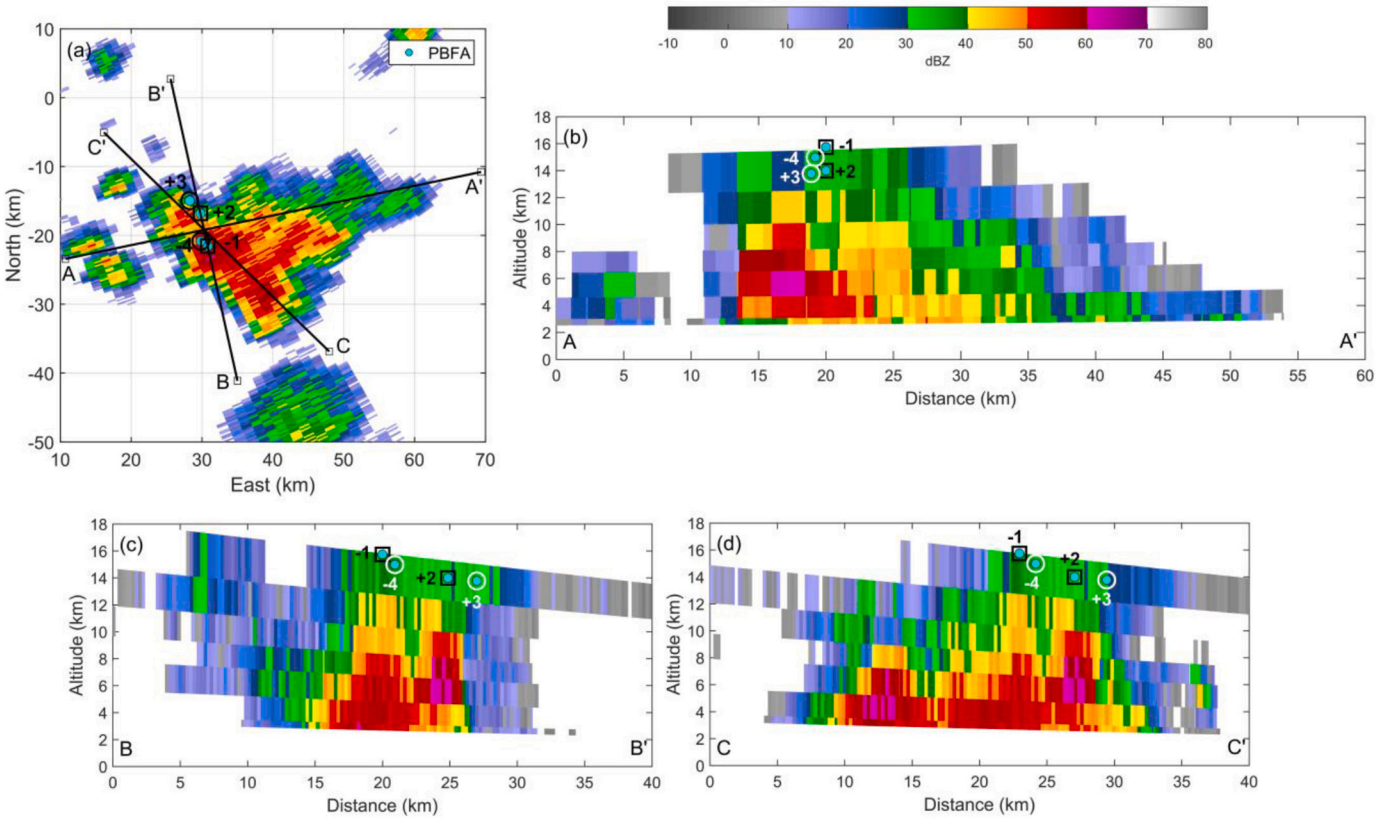

Fig. 5. Radar reflectivity along with NBEs shown in Fig. 4a. (a) NBEs from Groups 12 and 13 (numbered black circles) superimposed on PPI radar scan (3.4° elevation angle). Lines A–A′, B–B′, and C–C′ indicate the plan view locations of vertical radar cross-sections. (b) Vertical radar cross-section A–A', which passes through NBE-1 and NBE-2. (c) Vertical radar cross-section B–B′ is perpendicular to A–A' midway between NBE-1 and NBE-2. (d) Vertical radar along cross-section C–C′.

displaced by 5–10 km from the CG events.

6.3. Isolated NBE groups

As mentioned above, ten of the 15 NBE groups were Isolated. Fig. 4 shows data for two mixed polarity NBE groups (12 and 13) that were both "Isolated" spatiotemporally; each had one positive NBE and one negative NBE, and there were no other locatable lightning events within ±660 ms of these NBEs. Groups 12 and 13 were separated by only 3.5 s, so we discuss them together and label the NBEs of Group 12 as NBE-1 and NBE-2 and those of Group 13 as NBE-3 and NBE-4. As we will see, these two NBE groups were quite similar.

Fig. 4a shows that NBE-1 of Group 12 was a negative NBE and occurred 31 ms before NBE-2; these NBEs were separated horizontally by 4.9 km and vertically by 1.7 km. As shown in Fig. 4c and d, negative NBE-1 had E_{100km} and VHF power values of −2.43 V/m and 1020 W, while positive NBE-2 had a larger E_{100km} (8.35 V/m) and a smaller VHF power (884 W). Fig. 4b shows mixed polarity NBE Group 13, which had the positive NBE-3 first. The horizontal distance from NBE-3 to negative NBE-4 was 6.1 km and the time interval between the NBEs was 134 ms. Fig. 4e and f shows the positive NBE-3 had E_{100km} and VHF power values of 3.8 V/m and 814 W, while negative NBE-4 had smaller values (−0.5 V/m, 421 W).

In Fig. 5 the isolated NBE Groups 12 and 13 are superimposed the radar reflectivity data. The plan view (Fig. 5a) shows that the NBEs of both these groups occurred above storm regions with reflectivities >50 dBZ with the positive NBEs located north of the negative NBEs. The negative NBEs had location errors of dx ≤ 650 m, dy ≤480 m, and dz. ≤ 380 m, while the positive NBEs had smaller location errors, partly because they were closer to the sensor array. The vertical radar cross-section B-B′ (Fig. 5c) is aligned through the NBEs of Group 12 and nearly passes through the NBEs of Group 13 as well. Fig. 5c and d indicate that there were two vertical, high reflectivity cores (i.e., two thunderstorm cells) side by side, centered at about 20 km and 24 km on the horizontal distance axis of Fig. 5c (23 and 27 km on Fig. 5d). The two negative NBEs in Groups 12 and 13 both occurred above the taller reflectivity core (as indicated by the 40 dBZ contour) while the two positive NBEs of the groups occurred above the slightly lower, northern reflectivity core. Assuming that an upward-pointing electric field is needed to cause negative NBEs while a downward-pointing field is needed for positive NBEs, the electric field at the higher altitude above the taller reflectivity core apparently had opposite polarity to that slightly lower, above the shorter core; the opposite polarity fields were separated by only 4.9–6.1 km horizontally and 1–2 km vertically.

Fig. 6 shows another example of an Isolated NBE group, Group 8, which occurred in one of several fast-moving thunderstorms that occurred on August 26, 2016. Group 8 had two positive NBEs that occurred at altitudes of 13.8 km and 13.5 km. Fig. 6a shows 300 ms of FA and Log-RF data for NBE Group 8. There were no nearby lightning events within ±660 ms and 10 km, so Group 8 was Isolated. Fig. 6b and c show the FA and Log-RF waveforms of the two positive NBEs. Positive NBE-1 had a typical E_{100km} value (5.75 V/m) and a large VHF power (12,259 W), while positive NBE-2 had even larger values (15.1 V/m, 17,170 W). In Fig. 6d the Group 8 NBEs are superimposed on a low-level PPI scan from the Memphis radar; the storm was moving NNW roughly along the A-A' vertical cross section; the B-B′ cross section passes through the NBEs. As seen in Fig. 6e (A-A' cross section) the two positive NBEs were located above the storm's tilted core; storm motion was to the right in A-A'. The NBEs were found just above the radar echo and likely were within the cloud boundary. In Fig. 6e the tilted core had 30

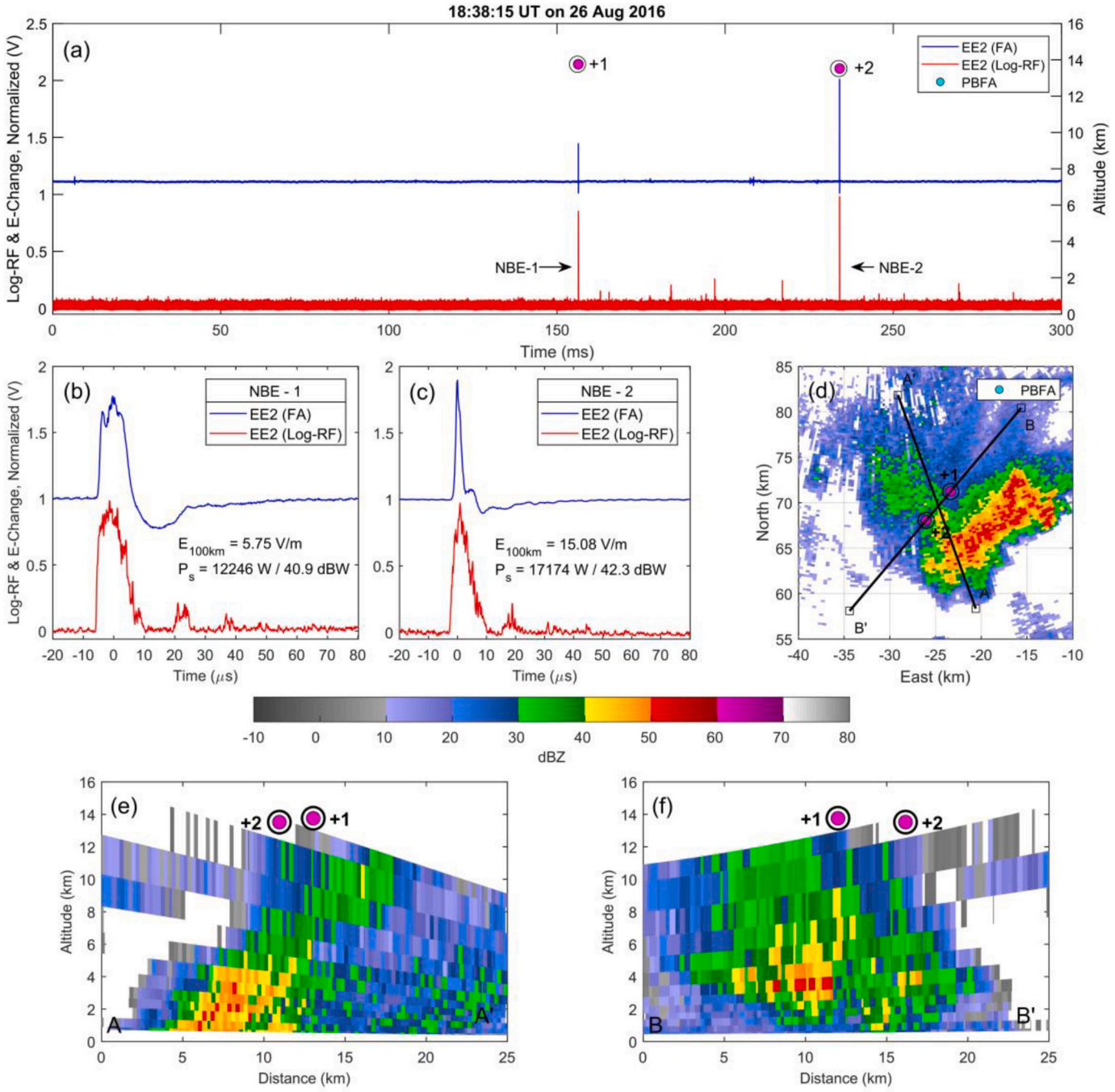

Fig. 6. Similar to Figs. 4 and 5, showing data for Group 8 of two positive NBEs that occurred in the anvil region of a storm. (a) FA, Log-RF, and altitude data for the two NBEs. (b), (c) Expanded views (100 μs) of FA and Log-RF data for the two NBEs. (d) PPI radar reflectivity showing NBEs and lines of vertical cross sections. (e) Vertical radar cross-section A–A'. Note that the uppermost radar beam shown was the highest scan (no radar data collected above this scan) (f) Vertical radar cross-section B–B′, which passes through NBE-1 and NBE-2.

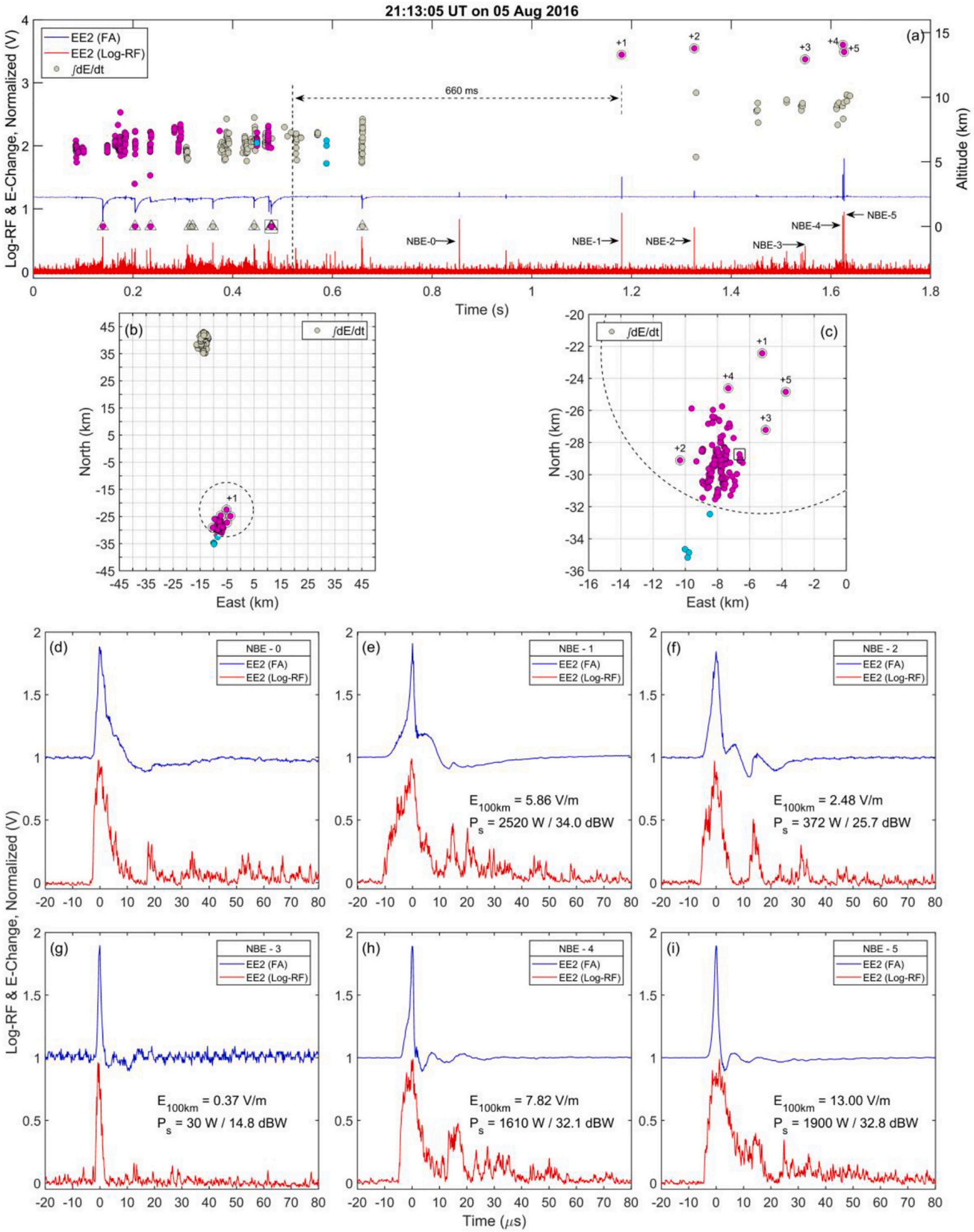

Fig. 7. Similar to Fig. 2, showing data for Group 11, five positive NBEs. Event locations are colored magenta, cyan, and gray if they are <10 km, 10–20 km, or >20 km, respectively, from NBE-1. (a) Overview showing 1.8 s of FA data (blue) and Log-RF data (red) including six positive NBEs and lightning pulses from two CG flashes and an IC flash. Triangles mark return strokes of the CG flashes. (b) Plan view of lightning locations shown in (a). Group 11 and one CG flash located in and beside the dashed, 10-km radius, circle centered on NBE-1 (magenta and cyan dots). A CG flash and an IC flash were located ~60 km north of NBE-1 (gray dots). (c) Expanded view of lightning events shown in (b) and located within 20 km of NBE-1. (d)-(i) Expanded views (100 μs) of FA and Log-RF data for the six NBEs. (For interpretation of the references to colour in this figure legend, the reader is referred to the web version of this article.)

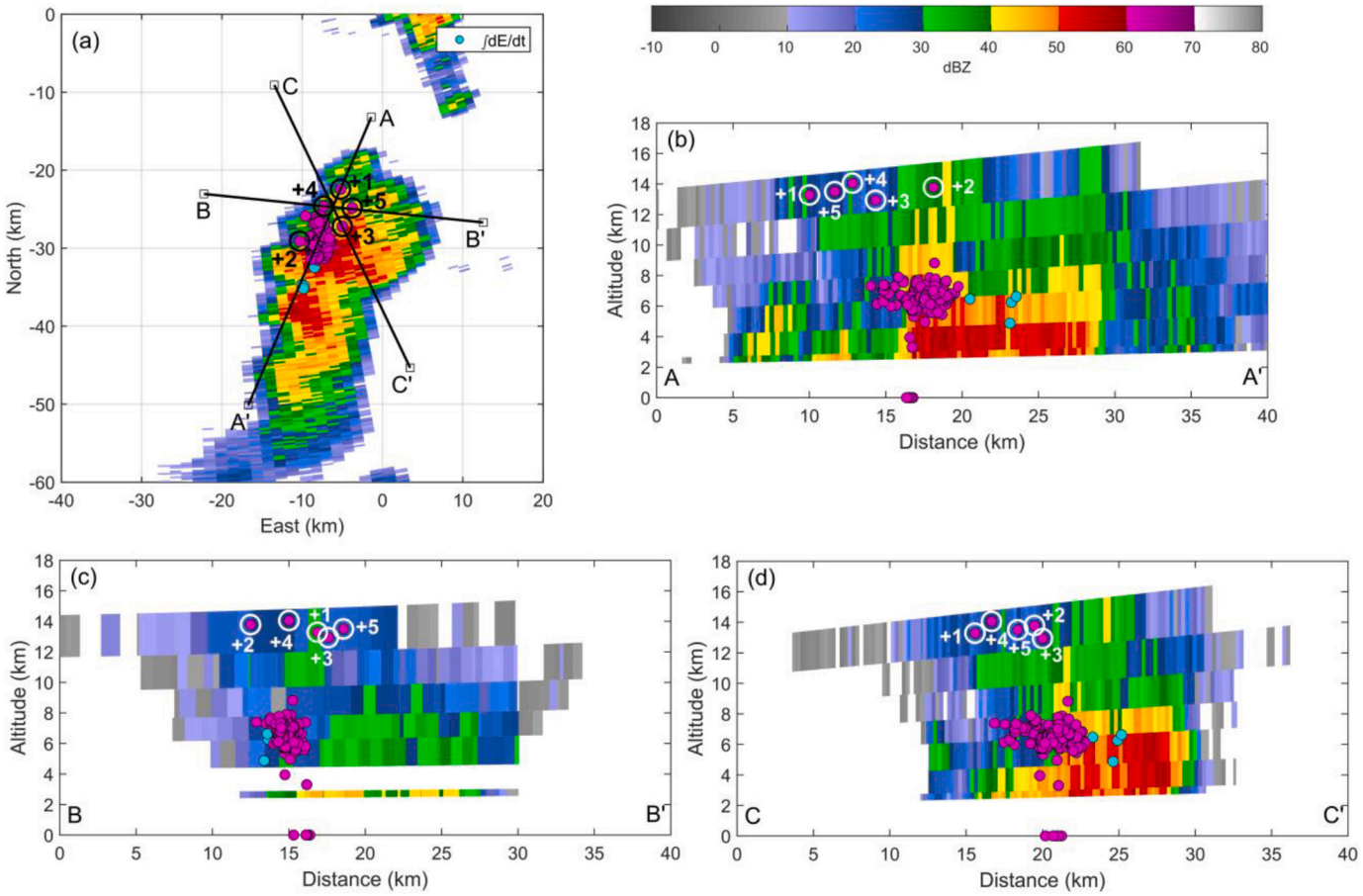

Fig. 8. Radar reflectivity along with NBEs and CG lightning events shown in Fig. 7(c). (a) NBEs (numbered black circles) and CG lightning events superimposed on PPI radar scan at 3.4° elevation angle. Lines A–A′, B–B′, and C–C′ indicate the plan view locations of the vertical radar cross-sections. (b) Vertical radar cross-section A–A', which passes through NBE-1. (c) Vertical radar cross-section B–B′, which passes through NBE-4 and NBE-5. (d) Vertical radar cross-section C–C′, which passes through NBE-3.

dBZ reflectivities extending to 12 km altitude and probably higher (but no data were available higher because the Memphis radar was only 40 km from the NBEs); these data suggest that the storm was quite vigorous. If the NBEs were within the cloud and below a negative screening layer, then the expected electric field would have been upward-pointing (which is opposite that needed to initiate positive NBEs). However, if the NBEs were just above the cloud boundary, then a substantial negative screening layer might have caused the downward-pointing electric field needed for positive NBEs. Fig. 6f verifies that the NBEs were close to the upper cloud boundary, but does not indicate exactly where the cloud boundary was.

Fig. 7 shows an example of an Isolated NBE group with five positive NBEs (Group 11) that occurred relatively close in space and time to two negative CG flashes (both with five return strokes) and one IC flash. NBE Group 11 occurred only 10 s before Group 2 (Figs. 2 and 3) and 17 min after Group 1 in the same storm. After locating almost all lightning pulses within ±660 ms of NBE-1, we categorized Group 11 as Isolated for reasons described below. In addition to the five located NBEs (labeled NBE-1 to NBE-5), another positive NBE (NBE-0) occurred about 300 ms before NBE-1, but we were unable to locate it. Fig. 7a shows 1.8 s of FA and Log-RF data along with altitudes of lightning events that included the five NBEs, two CG flashes and one IC flash. (Note that return strokes are plotted at z = 0 km using altitude axis on right in Fig. 1a.) The lightning events are shown as magenta, cyan, and gray dots respectively for events <10 km, 10–20 km, and > 20 km horizontally from NBE-1. NBEs are indicated by numbered circles while return strokes are marked with triangles. The two CG flashes overlapped in time and occurred before Group 11, and the IC flash was concurrent with NBE Group 11. The plan view of the events (Fig. 7b) shows that one of the CG flashes and the IC flash were ~ 60 km north of Group 11 and the other CG flash. The northern CG flash and the IC flash were in a separate thunderstorm from Group 11.

The plan view of NBE Group 11 and the nearby CG flash is shown in more detail in Fig. 7c. The first stroke of the CG flash occurred 1040 ms before and 6.9 km horizontally from NBE-1. The last return stroke (marked with a square in Fig. 7a and c) occurred 703 ms before and 6.5 km from NBE-1, while the last four events of this flash occurred about 600 ms before NBE-1 and slightly outside the 10 km radius from NBE-1 (four cyan dots). These events are <10 km from, but occur >660 ms before, NBE-2 and NBE-3. Thus, Group 11 was categorized as "Isolated." However, it is clear that the thunderstorm region that produced the NBEs of Group 11 was strongly electrified with at least five volumes with the very large electric field conditions needed for initiating positive NBEs. In addition, within the next 11 s, the same thunderstorm region produced two more positive NBEs, i.e. Group 2, indicating conditions similar to those for the NBE "recurrent sets" studied by Karunarathna et al. (2015).

Expanded views (100 μs) of all six NBEs, along with range-normalized FA amplitude (E_{100km}) and Log-RF power for located NBEs, are shown in Figs. 7(d)-7(i). E_{100km} values of the five NBEs of Group 11 were, respectively, 5.9, 2.5, 0.4, 7.8, and 13.0 V/m; Log-RF powers were, respectively, 2520, 370, 30, 1610, and 1910 W; and altitudes were, respectively, 13.3, 13.8, 12.9, 14.1 and 13.5 km.

Fig. 8 shows radar reflectivity data associated with the NBE Group

Table 5
NBE locations relative to thunderstorm radar reflectivity locations[a].

Group #	Group type	NBE polarity	NBE altitudes (km)[b]	NBE locations relative to radar reflectivity
1	Isolated	positive	12.9	#1 beside core
		positive	13.3	#2 high in anvil
2	Not-Isolated	positive	13.6	#1 high in anvil
	(10.3 s after	positive	13.5	#2 high in anvil
	Group 11)			Fig. 3
3	Isolated	positive	14.2	#1 high in anvil
		positive	15.3	#2 high in anvil
4	Not-Isolated	positive	15.2	#1 above core
		positive	13.7	#2 high in anvil
5	Isolated	positive	15.2	#1 high above core
		positive	14.6	#2 high above core
6	Isolated	positive	11.1	#1 in core
	(71.7 s after	positive	10.1	#2 in core
	Group 10)			
7	Isolated	positive	11.9	#1 in core
	(106.3 s after	positive	10.6	#2 in core
	Group 6)			
8	Isolated	positive	13.8	#1 high above core
		positive	13.5	#2 high above core
				Fig. 6
9	Isolated	positive	11.4	#1 in core
		positive	13.5	#2 in core
10	Not-Isolated	positive	14.4	#1 above core
		positive	10.1	#2 in core
		positive	12.7	#3 in core (above CG IB pulses)
11	Isolated	positive	13.3	#1 high in anvil
	(16 min, 56.7 s	positive	13.8	#2 in upper core
	after Group 1)	positive	12.9	#3 beside core
		positive	14.1	#4 high in anvil
		positive	13.5	#5 high in anvil
				Fig. 8
12	Isolated	negative	15.7	#1 above one core
		positive	14.0	#2 above another core
				Fig. 5
13	Isolated	positive	13.8	#1 above one core
	(3.4 s after	negative	15.0	#2 above another core
	Group 12)			Fig. 5
14	Not-Isolated	positive	13.2	#1 above sheared core
		negative	12.7	#2 above sheared core
15	Not-Isolated	positive	14.8	#1 high above core
	(21.1 s after	negative	7.4	#2 low in core
	Group 4)	positive	13.9	#3 high in anvil

[a] Radar locations: "in or above thunderstorm core," "beside thunderstorm core," and "in thunderstorm anvil," as defined by Karunarathna et al. (2015).
[b] NBEs listed in order of occurrence time.

11. (The radar data are the same as used for Fig. 3 since NBE Groups 2 and 11 were separated in time by only 10 s.) The five NBEs of Group 11 occurred within 31 km of the central sensor site and had location errors of dx $\leq$ 70 m, dy $\leq$180 m, and dz. $\leq$ 260 m. Fig. 8a shows the NBEs and the CG lightning events from Fig. 7c superimposed on a PPI radar reflectivity scan. Vertical radar cross sections are shown in Fig. 8b, c, and d, respectively; cell motion was approximately toward C in Fig. 8d. Each NBE is shown as a numbered circle. All these positive NBEs occurred in the upper part of the cloud, while the located lightning events of the negative CG flash were below 8 km altitude in or near the storm core with >30 dBZ reflectivity (Fig. 8b). NBE-2 and NBE-3 occurred just beside the main reflectivity core, in 25–30 dBZ (Fig. 8b and d, respectively), while NBE-1, NBE-4, and NBE-5 occurred high in the downshear anvil, in reflectivities of 20–30 dBZ (Fig. 8b and d,). As already discussed for NBE Group 2 (Fig. 3), the storm had a vigorous updraft with 40 dBZ reflectivity extending up to altitudes of ~13.5 km (Fig. 8b and d). Similar to Group 2, we speculate that the occurrence of numerous NBEs in NBE Group 11 was related to its dynamic intensity.

General storm locations based on the nearby radar structure for all NBE groups, including the Isolated NBE groups not discussed above, are listed in Table 5.

7. Discussion

In this section we discuss several aspects of the data presented above. As mentioned already, we found no INBE groups; i.e., none of the NBEs in the 15 NBE groups initiated a CG or an IC flash. This result means that the groups of NBEs were not a series of attempted flash initiations that eventually started a flash, although the negative NBE in Group 15 was apparently a precursor of a CG flash that initiated 25 ms later. Using an altitude histogram of NBEs, Wu et al. (2014) showed that 94% of 103 positive INBEs in Japanese thunderstorms occurred at altitudes <10 km, while 98% of 535 typical positive NBEs and 100% of 189 high-altitude negative NBEs occurred at altitudes >10 km. We found that the altitude histogram of 146 positive NBEs in Mississippi thunderstorms (Fig. 9a, data from Bandara et al., 2020) was quite similar to the altitude histogram in Wu et al. (2014), except that a few more INBEs in Mississippi thunderstorms occurred above 10 km altitude. Fig. 9b gives the altitude histogram of the 31 positive NBEs in NBE Groups from the present study and shows that all positive NBEs in NBE groups occurred at altitudes >10 km, where positive INBEs rarely occur. Perhaps the lack of INBE groups suggests that the regions of large electric field needed to cause the NBEs in NBE groups were too small to support a full IC flash.

As discussed above in Section 4, earlier NBE(s) in an NBE group did not seem to initiate later NBEs in the group, a conclusion that was based on the finding that $E_{1\text{-}2}$ between successive pairs of NBEs was too small. In Section 5 we found that during the time of most NBE groups, there were many more EAS cosmic rays passing through the overall NBE group volume than the number of NBEs in the group, suggesting that the NBEs of a group only occurred in smaller volumes of ~1 km^3 containing many smaller regions with E $\geq$ 3 MV/(m·atm) (needed to start the swarm of positive streamers that comprise each NBE). Thus, we conclude that the ten Isolated NBE groups (with 2 or 5 NBEs) had, almost simultaneously, two or five small regions with an electric field sufficiently large to cause the individual NBEs. Similarly, the five Not-Isolated NBE groups (with either 2 or 3 NBEs) had, almost simultaneously, two or three small regions with electric fields large enough to cause the NBEs, in addition to having another region with a large electric field magnitude in a more extensive volume needed to cause the full lightning flash that made the NBE group be Not-Isolated. Brothers et al. (2018) modeled thunderstorm charge regions and found that charge advection and associated turbulence causes small volumes with large charge densities of opposite polarity near a storm's updraft, as shown in Fig. 10. The small charge volumes in Fig. 10 are consistent with the discussion in Section 5 of an individual NBE volume of ~1 km^3; the 1 km^3 volume contains the smaller E_{th}-volumes with E $\geq$ 3 MV/(m·atm) to start the positive streamers of the NBE.

To help with the understanding of Fig. 10, Fig. 11 depicts the updraft in a small New Mexico thunderstorm, showing radar reflectivity and 3D wind vectors (from Stolzenburg and Marshall, 1998). Note, however, that the storm shown in Fig. 10 and the Mississippi thunderstorms with NBE groups were taller, had greater horizontal extent, and presumably had more substantial updrafts than the small New Mexico storm depicted in Fig. 11. In Fig. 11 the storm updraft core was oriented nearly vertically (between 0 and 1.5 km on horizontal axis) with a maximum speed of 12 m/s; the reflectivity core ($\geq$ 30 dBZ) was located between −2 and 0.5 km on the horizontal axis and extended upward to about 9.5 km altitude, so the updraft was adjacent to and overlapping with the reflectivity core. Based on Brothers et al. (2018), the updraft in Fig. 11 should have caused small regions of large electric field that were also in the vicinity of the reflectivity core. Assuming that similar, small charge regions were produced in the Mississippi thunderstorms in the vicinity of the thunderstorm updraft and high reflectivity core, it is not surprising

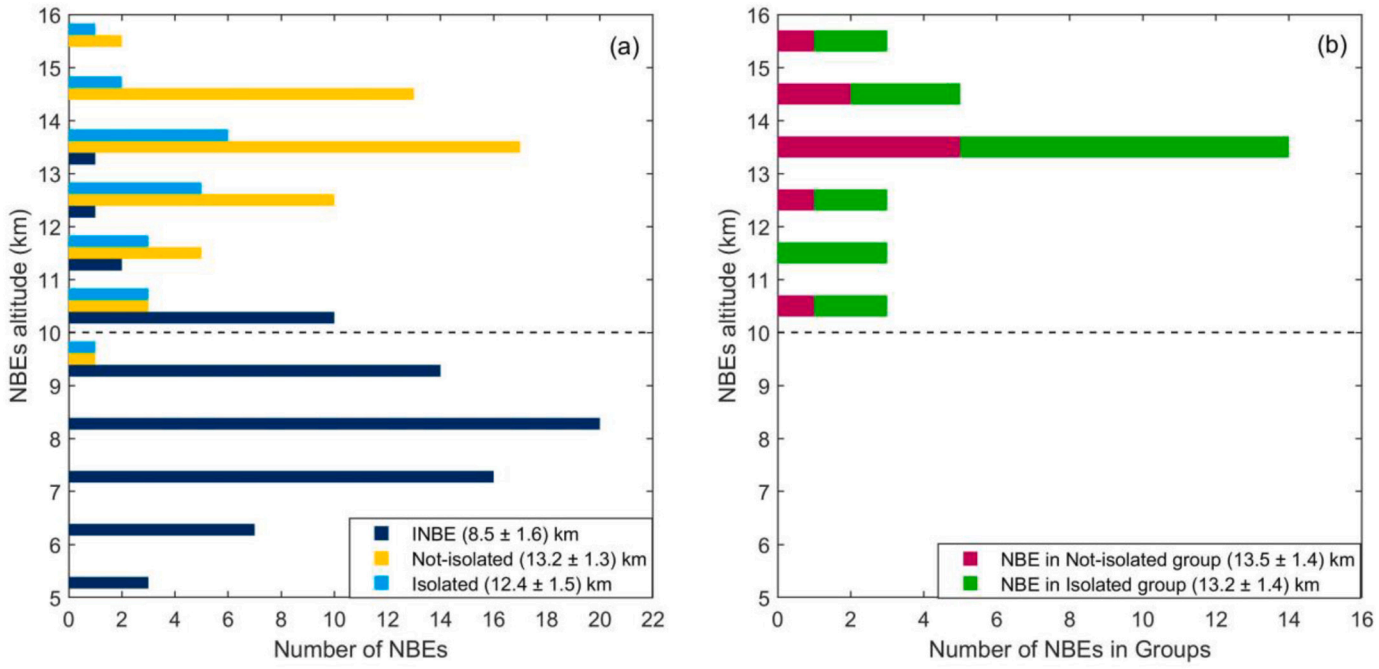

Fig. 9. (a) Altitude histogram of 146 positive NBEs from Bandara et al. (2020), including 74 INBEs, 51 Not-Isolated NBEs, and 21 Isolated NBEs. (b) Altitude histogram of all 31 positive NBEs from NBE Groups of this paper, including 10 Not-Isolated NBEs, and 21 Isolated NBEs. It is important to remember that all of the NBEs in (b) would be "not-isolated" if plotted as in (a), since the definition of an NBE group means that the NBEs in the group are not-isolated from other NBEs in the group. For this reason, the data in (b) are "stacked" in the histogram. For both histograms the average and standard deviation altitudes are given parenthetically in the figure legends.

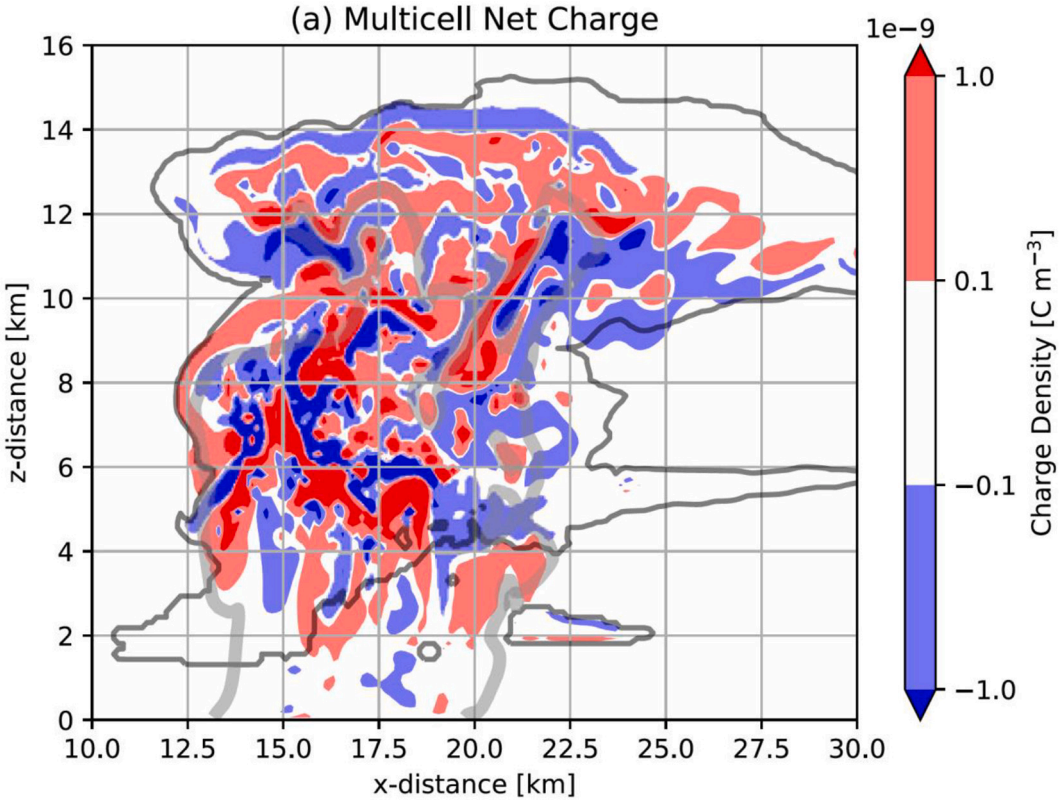

Fig. 10. Vertical cross section of a multi-cell thunderstorm showing modeled charge regions superimposed on the cloud boundary (thin dark gray line), after Fig. 4(a) in Brothers et al. (2018). Red regions denote positive charge with blue regions for negative charge. The 35 dBZ reflectivity contour is shown as a thick, light gray line. Very approximately, the storm updraft moved upward from (x, z) location of (14, 1) to (18, 13). (For interpretation of the references to colour in this figure legend, the reader is referred to the web version of this article.)

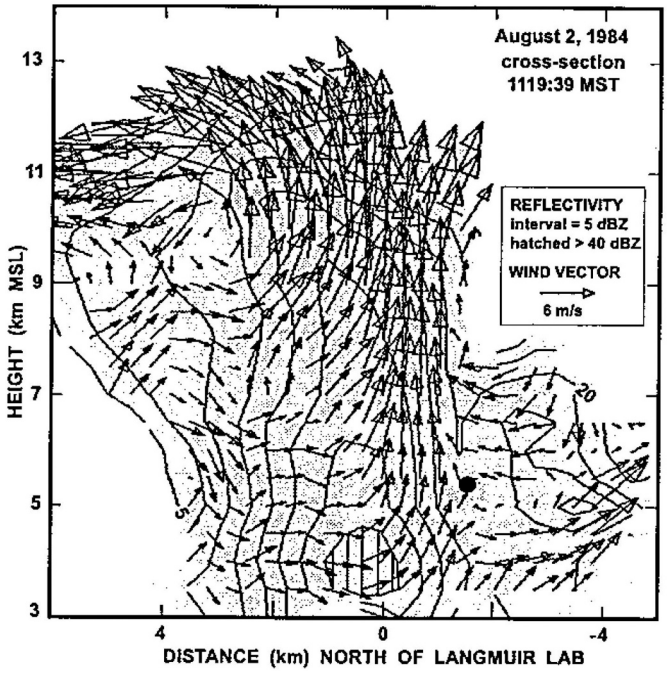

Fig. 11. Vertical radar cross-section of a New Mexico mountain thunderstorm with particle wind speed vectors superimposed. Reflectivity contours shown every 5 dBZ with 5 and 20 dBZ contours are marked; small hatched region near bottom center denotes reflectivity >40 dBZ. The storm updraft moved upward almost vertically between 0 and 1.5 km on horizontal axis; the reflectivity core >30 dBZ is located between +2 and –0.5 km on the horizontal axis and extends upward to about 9.5 km altitude. (After Fig. 4 in Stolzenburg and Marshall (1998).)

that 23 of the 35 NBEs in NBE groups occurred in or above the reflectivity core (Table 4). Large electric field magnitudes have been observed at high altitudes in thunderstorm convection: Stolzenburg and Marshall (2009) show five cases from a set of 50 balloon soundings in which E values were near or in excess of the runaway breakdown threshold value above 12 km altitude.

Fig. 12 compares the FA amplitude (E_{100km}) and the VHF power (from Log-RF sensor) of the 35 NBEs in NBE groups. The general trend in Fig. 12 was for larger E_{100km} values to be associated with larger VHF powers, with a Spearman rank correlation coefficient, ρ, of 0.72 for the positive NBEs. However, weak E_{100km} values (< 2.5 V/m) did not follow this trend, since over the 0–2.5 V/m range the VHF powers of both positive and negative NBEs varied widely, from 30 W to 3480 W. Bandara et al. (2020) found a much weaker correlation, $\rho = 0.33$, between the FA E_{100km} amplitude and the VHF power of 192 positive NBEs. A lack of correlation is not necessarily surprising since the FA measures longer charge motions (> 120 m) than the VHF sensor (~1.6 m), as discussed in Bandara et al. (2020).

8. Summary and conclusions

We have analyzed 35 NBEs that occurred in 15 groups in Mississippi thunderstorms; there were 31 positive NBEs and four negative NBEs, and the NBE groups had 2, 3, or 5 NBEs. There were four NBE groups with both positive and negative NBEs. By our definition a NBE group occurred when one NBE was preceded or followed by one or more NBEs located within a 10 km horizontal radius (Δh) and a ± 660 ms time interval (ΔT). Table 1 lists the 15 NBE groups and shows how each satisfied the Δh and ΔT requirements.

For each NBE in the NBE groups, Table 2 gives the NBE's range-normalized fast antenna amplitude (E_{100km}) and its VHF power (from Log-RF sensors). Many of the 35 NBEs in the NBE groups had typical E_{100km} values and typical VHF powers. However, 17 NBEs had a small FA amplitude, $|E_{100km}| \leq 2.5$ V/m, and 7 NBEs had a small VHF power (≤ 100 W). The 7 low-power NBEs also had especially small FA amplitudes, $|E_{100km}| < 1.0$ V/m. These findings suggest that NBEs with small FA amplitude and/or low VHF power, found herein because of their occurrence in a NBE group, may be more prevalent that previously realized.

Since NBEs sometimes initiate IC flashes and CG flashes (e.g., Rison et al., 1999; Wu et al., 2014; Rison et al., 2016; Bandara et al., 2019), in Section 4 we investigated whether the first NBE in a group likely had initiated the second NBE, and if the second NBE had initiated by the third NBE, etc. With one possible exception, we found that successive NBE pairs in the 15 NBE groups were too far separated in space for the earlier NBE to have initiated the later NBE. Thus, each NBE in the NBE groups initiated independently, so each NBE required a pre-existing large magnitude, local electric field.

In Section 5 we showed (see Table 3) that the data of the NBE groups are consistent with the turbulence-EAS/RREA mechanism for making NBEs (Kostinskiy et al., 2020a). The turbulence-EAS/RREA mechanism states that each NBE occurs in a separate 1 km^3 volume containing many small regions with electric field ≥3 MV/(m·atm); an EAS/RREA passing through the 1 km^3 volume initiates the positive streamers that make up the NBE. The analysis in Section 5 also indicates that the whole volume associated with the NBEs of a group did not have E ≥ 3 MV/(m·atm).

In Section 6 the 15 NBE groups were categorized spatiotemporally relative to non-NBE lightning events into one of three types: Isolated, Not-Isolated, and INBE (meaning an NBE in the group initiated a lightning flash). The spatiotemporal results are shown in Table 4; 10 NBE groups were Isolated from other lightning events, 5 NBE groups were Not-Isolated, and zero NBE groups initiated a lightning flash. For the five Not-Isolated groups, none of the IC or CG lightning events that occurred within 660 ms and 10 km horizontally of the NBEs initiated any of the NBEs. Thus each NBE in an NBE group initiated independently of other NBEs and of other lightning events within ±660 ms and 10 km horizontally of the NBE.

The NBE groups were placed into the radar reflectivity structure of their parent thunderstorms, and the results are summarized in Table 5. All 35 NBEs occurred within or just above the cloud radar echo boundary. Most (23) of the 35 NBEs in groups occurred in or above the storm's high reflectivity core where, according to the modeling of Brothers et al. (2018), there are many small volumes with large charge densities (both positive and negative). Contiguous, oppositely charged volumes would produce the small regions with large electric fields needed to initiate the NBEs in groups. We speculate that the occurrence NBE groups is often associated with dynamically intense convection. Another storm locale where small regions with large electric fields might be found is high in anvils, where screening charge layers also contribute to complexity in the electrical structure. Ten of the 31 positive NBEs in the NBE groups occurred high in a thunderstorm anvil, where it is generally thought that normal lightning initiation is less frequent and where the large-scale electric field is expected to be upward-pointing instead of the downward-pointing field needed for a positive NBE. Karunarathna et al. (2015) also found positive NBEs in the high anvil of thunderstorms in Florida, and their work suggested turbulence as a primary way in which the small-scale electric field in a thunderstorm anvil might be downward pointing.

Overall, this study of NBE groups provides new data on the locations of NBEs relative to thunderstorm radar reflectivity structure, on weak NBEs, on the physical independence of each NBE from other NBEs in the same group, on the volume of individual NBEs, and on the physical mechanism of NBEs. This study also gives support to the turbulence-EAS/RREA mechanism suggested by Kostinskiy et al. (2020a) for the initiation and development of NBEs.

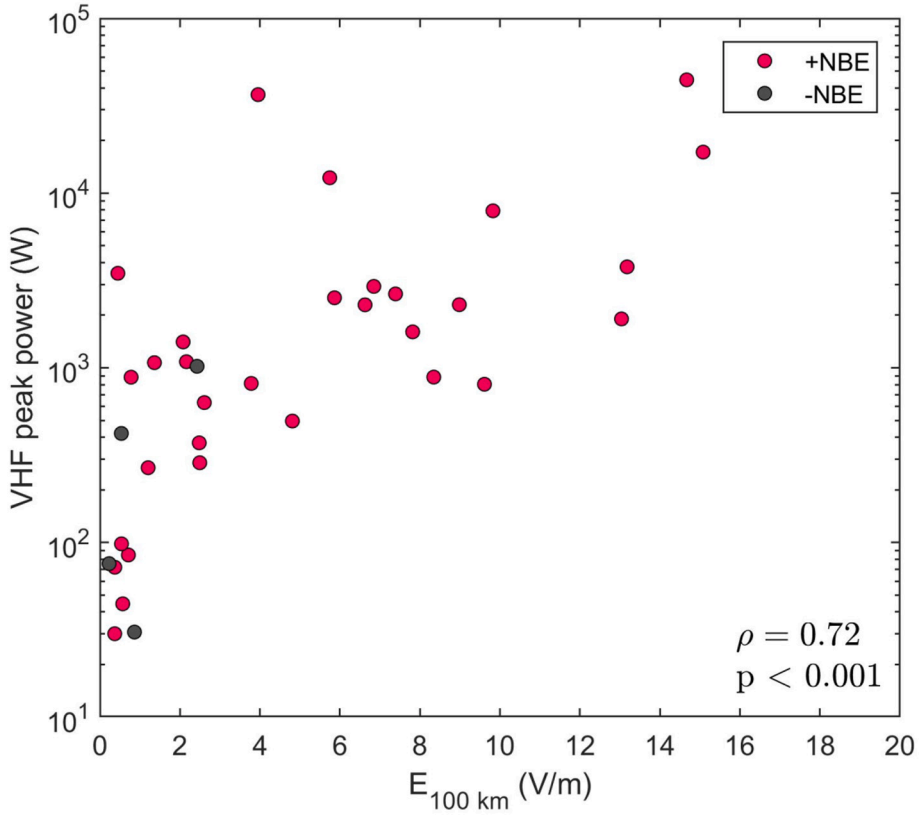

Fig. 12. Scatter plot of VHF peak power (Log-RF) versus peak FA amplitude, range normalized to 100 km, for 35 NBEs from NBE groups. ρ = Spearman correlation coefficient. p = probability value.

Declaration of Competing Interest

None.

Acknowledgements

We appreciate the support of the sensor site hosts: University of Mississippi Electrical Engineering Department, University of Mississippi Field Station, Jan Murray, Scott and Cherry Watkins, Bill and Crystal MacKenzie, and Martha Mills and the North Delta School. We are grateful for the constructive suggestions of the reviewers. Research data used herein are available directly from the corresponding author. This work was supported by US National Science Foundation grants AGS-1532038 and AGS-1742930, and it comprises a portion of the PhD dissertation research of the lead author.

References

Attanasio, A., Krehbiel, P.R., da Silva, C.L., 2019. Griffiths and Phelps lightning nitiation model, revisited. Journal of Geophysical Research: Atmospheres 124, 8076–8094. https://doi.org/10.1029/2019JD030399.

Babich, L.P., Bochkov, E.I., Kutsyk, I.M., Neubert, T., Chanrion, O., 2016. Positive streamer initiation from raindrops in thundercloud fields. J. Geophys. Res. Atmos. 121, 6393–6403. https://doi.org/10.1002/2016JD024901.

Bandara, S., Marshall, T., Karunarathne, S., Karunarathne, N., Siedlecki, R., Stolzenburg, M., 2019. Characterizing three types of negative narrow bipolar events in thunderstorms. Atmos. Res. 227, 263–279. https://doi.org/10.1016/j.atmosres.2019.05.013.

Bandara, S., Marshall, T., Karunarathne, S., Stolzenburg, M., 2020. Electric field change and VHF waveforms of positive Narrow Bipolar events in Mississippi thunderstorms. Atmos. Res. 243 https://doi.org/10.1016/j.atmosres.2020.10500.

Bils, J.R., Thomson, E.M., Uman, M.A., Mackerras, D., 1988. Electric field pulses in close lightning cloud flashes. J. Geophys. Res. 93 (D12), 15,933–15,940.

Brothers, M.D., Bruning, E.C., Mansell, E.R., 2018. Investigating the Relative Contributions of Charge Deposition and Turbulence in Organizing Charge within a Thunderstorm. J. Atmos. Sci. 75, 3265–3284. https://doi.org/10.1175/JAS-D-18-0007.1.

Byrne, G.J., Few, A.A., Stewart, M.F., 1989. Electric field within a severe thunderstorm anvil. J. Geophys. Res. 94 (D5), 6297–6307. https://doi.org/10.1029/JD094iD05p06297.

Karunarathna, N., Marshall, T.C., Stolzenburg, M., Karunarathne, S., 2015. Narrow bipolar pulse locations compared to thunderstorm radar echo structure. J. Geophys. Res. 120 (22), 11,690–11,706. https://doi.org/10.1002/2015JD023829.

Karunarathne, S., Marshall, T.C., Stolzenburg, M., Karunarathna, N., Vickers, L.E., Warner, T.A., Orville, R.E., 2013. Locating initial breakdown pulses using electric field change network. Journal of Geophysical Research Atmospheres 118 (13), 7129–7141. https://doi.org/10.1002/jgrd.50441.

Karunarathne, S., Marshall, T.C., Stolzenburg, M., Karunarathna, N., 2015. Observations of positive narrow bipolar pulses. J. Geophys. Res. 120 (14), 7128–7143. https://doi.org/10.1002/2015JD023150.

Karunarathne, S., Marshall, T.C., Stolzenburg, M., Karunarathna, N., 2016. Electrostatic field changes and durations of narrow bipolar events. J. Geophys. Res. Atmos. 121, 10,161–10,174. https://doi.org/10.1002/2016JD024789.

Kostinskiy, A., Marshall, T., Stolzenburg, M., 2020a. The mechanism of the origin and development of lightning from initiating event to initial breakdown pulses (v.2). Journal of Geophysical Research: Atmospheres 125. https://doi.org/10.1029/2020JD033191.

Kostinskiy, A.Yu., Vlasov, A., Fridman, M., 2020b. Calculation of the dynamics of the initiation of streamer flashes that provide the NBE VHF signal profile and the VHF phase wave propagation velocity arXiv: 2005.12417 v1 [physics.ao-ph].

Le Vine, D.M., 1980. Sources of the strongest RF radiation from lightning. J. Geophys. Res. 85 (C7), 4091–4095.

Lyu, F., Cummer, S.A., Qin, Z., Chen, M., 2019. Lightning initiation processes imaged with very high frequency broadband interferometry. Journal of Geophysical Research: Atmospheres 124. https://doi.org/10.1029/2018JD029817.

Marshall, T., Schulz, W., Karunarathna, N., Karunarathne, S., Stolzenburg, M., Vergeiner, C., Warner, T., 2014. On the percentage of lightning flashes that begin with initial breakdown pulses. J. Geophys. Res. Atmos. 119, 445–460. https://doi.org/10.1002/2013JD020854.

Marshall, T., Bandara, S., Karunarathne, N., Karunarathne, S., Kolmasova, I., Siedlecki, R., Stolzenburg, M., 2019. A study of lightning flash initiation prior to the first initial breakdown pulse. Atmos. Res. 217, 10–23. https://doi.org/10.1016/j.atmosres.2018. 10.013.

Marshall, T.C., Rust, W.D., Winn, W.P., Gilbert, K.E., 1989. The electrical structure in two thunderstorm anvil clouds. J. Geophys. Res. 94 (D2), 2171–2181. https://doi.org/10.1029/JD094iD02p02171.

Nag, A., Rakov, V.A., Tsalikis, D., Cramer, J.A., 2010. On phenomenology of compact intracloud lightning discharges. J. Geophys. Res. 115 (D14), D14115 https://doi.org/10.1029/2009JD012957.

Rison, W., Thomas, R.J., Krehbiel, P.R., Hamlin, T., Harlin, J., 1999. A GPS-based three-dimensional lightning mapping system: initial observations in Central New Mexico. Geophys. Res. Lett. 26 (23), 3573–3576. https://doi.org/10.1029/1999GL010856.

Rison, William, Krehbiel, P.R., Stock, M.G., Edens, H.E., Shao, X.-M., Thomas, R.J., Zhang, Y., 2016. Observations of narrow bipolar events reveal how lightning is initiated in thunderstorms. Nature Communications 7 (1), 10721. https://doi.org/10.1038/ncomms10721.

Rutjes, C., Ebert, U., Buitink, S., Scholten, O., Trinh, T.N.G., 2019. Generation of seed electrons by extensive air showers, and the lightning inception problem including narrow bipolar events. Journal of Geophysical Research: Atmospheres 124, 7255–7269. https://doi.org/10.1029/2018JD029040.

Smith, D.A., Shao, X.M., Holden, D.N., Rhodes, C.T., Brook, M., Krehbiel, P.R., Thomas, R.J., 1999. A distinct class of isolated intracloud lightning discharges and their associated radio emissions. Journal of Geophysical Research: Atmospheres 104 (D4), 4189–4212. https://doi.org/10.1029/1998JD200045.

Smith, D.A., Eack, K., Harlin, J., Heavner, M., Jacobson, A., Massey, R., Shao, X., Wiens, K., 2002. The Los Alamos Sferic Array: a research tool for lightning investigations. J. Geophys. Res. 107 (D13), 4183. https://doi.org/10.1029/2001JD000502.

Smith, D.A., Heavner, M.J., Jacobson, A.R., Shao, X.M., Massey, R.S., Sheldon, R.J., Wiens, K.C., 2004. A method for determining intracloud lightning and ionospheric heights from VLF/LF electric field records. Radio Science 39 (1). https://doi.org/10.1029/2002RS002790 n/a-n/a.

Stolzenburg, M., Marshall, T.C., 1998. Charged precipitation and electric field in two thunderstorms. J. Geophys. Res. 103, 19,777–19,790.

Stolzenburg, M., Marshall, T.C., 2008. Charge structure and dynamics in thunderstorms, Space Sci. Rev. 137, 355–372. https://doi.org/10.1007/s11214-008-9338-z.

Stolzenburg, M., and T. C. Marshall (2009), Electric field and charge structure in lightning-producing clouds, Lightning: Principles, Instruments and Applications, H.-D. Betz, U. Schumann, P. Laroche (Eds.), 641 pp., Springer, doi: https://doi.org/10.1007/978-1-4020-9079-0_3.

Stolzenburg, M., Marshall, T.C., Krehbiel, P.R., 2010. Duration and extent of large electric fields in a thunderstorm anvil cloud after the last lightning. J. Geophys. Res. 115, D19202 https://doi.org/10.1029/2010JD014057.

Stolzenburg, M., Marshall, T.C., Karunarathne, S., Karunarathna, N., Vickers, L.E., Warner, T.A., Orville, R.E., Betz, H.-D., 2013. Luminosity of initial breakdown in lightning. J. Geophys. Res. Atmos. 118, 2918–2937. https://doi.org/10.1002/jgrd.50276.

Tilles, J.N., Liu, N., Stanley, M.A., Krehbiel, P.R., Rison, W., Stock, M.G., et al., 2019. Fast negative breakdown in thunderstorms. Nat. Commun. 10, 1648. https://doi.org/10.1038/s41467-019-09621-z.

Wiens, K.C., Hamlin, T., Harlin, J., Suszynsky, D.M., 2008. Relationships among Narrow Bipolar events, "total" lightning, and radar-inferred convective strength in Great Plains thunderstorms. Journal of Geophysical Research Atmospheres 113 (5), 1–31. https://doi.org/10.1029/2007JD009400.

Willett, J.C., Bailey, J.C., Krider, E.P., 1989. A class of unusual lightning electric field waveforms with very strong high-frequency radiation. J. Geophys. Res. 94 (D13), 16255. https://doi.org/10.1029/JD094iD13p16255.

Wu, T., Dong, W., Zhang, Y., Funaki, T., Yoshida, S., Morimoto, T., Kawasaki, Z., 2012. Discharge height of lightning narrow bipolar events. Journal of Geophysical Research: Atmospheres 117 (D5). https://doi.org/10.1029/2011JD017054 n/a-n/a.

Wu, T., Takayanagi, Y., Yoshida, S., Funaki, T., Ushio, T., Kawasaki, Z., 2013. Spatial relationship between lightning narrow bipolar events and parent thunderstorms as revealed by phased array radar. Geophys. Res. Lett. 40 (3), 618–623. https://doi.org/10.1002/grl.50112.

Wu, T., Yoshida, S., Ushio, T., Kawasaki, Z., Wang, D., 2014. Lightning-initiator type of narrow bipolar events and their subsequent pulse trains. Journal of Geophysical Research: Atmospheres 119 (12), 7425–7438. https://doi.org/10.1002/2014JD021842.